EUROPEAN HEMATOLOGY ASSOCIATION

haematologica
Journal of the European Hematology Association

LEF-1 drives aberrant β-catenin nuclear localization in myeloid leukemia cells

by Rhys G Morgan, Jenna Ridsdale, Megan Payne, Kate J Heesom, Marieangela C Wilson, Andrew Davidson, Alexander Greenhough, Sara Davies, Ann C Williams, Allison Blair, Marian L Waterman, Alex Tonks, and Richard L Darley

Manuscript title: LEF-1 drives aberrant β-catenin nuclear localization in myeloid leukemia cells

Running title: LEF-1 regulates β-catenin nuclear localization

Article type: Original article

Authors/Affiliations: Rhys G Morgan[1,2]*, Jenna Ridsdale[3], Megan Payne[1], Kate J Heesom[4], Marieangela C Wilson[4], Andrew Davidson[1], Alexander Greenhough[1], Sara Davies[3], Ann C Williams[1], Allison Blair[1], Marian L Waterman[5], Alex Tonks[3], Richard L Darley[3]*

[1] School of Life Sciences, University of Sussex, John Maynard Smith Building, Brighton, BN1 9QG, UK.
[2] School of Cellular and Molecular Medicine, University of Bristol, Biomedical Sciences Building, Bristol, BS8 1TD, UK.
[3] Department of Haematology, Division of Cancer & Genetics, School of Medicine, Cardiff University, Cardiff, CF14 4XN, UK.
[4] University of Bristol Proteomics Facility, Biomedical Sciences Building, University Walk, Bristol, BS8 1TD, UK.
[5] Department of Microbiology and Molecular Genetics, University of California Irvine, Irvine, CA, USA.

*Corresponding authors:

Prof. Richard Darley, Department of Haematology, Division of Cancer and Genetics, School of Medicine, Cardiff University, Cardiff, CF14 4XN, UK.

Email: darley@cardiff.ac.uk

Tel: +442920745507

Dr. Rhys Morgan, School of Life Sciences, University of Sussex, John Maynard Smith Building, Brighton, BN1 9QG, UK.

Email: rhys.morgan@sussex.ac.uk

Tel: +441273877861

Word counts: Main text 4294, Abstract 194

Figures/tables: 8

References: 56

Supplementary material: 9 figures, 3 tables (plus supplementary methods and mass spec datasets)

Article summary

- The aim of this study was to investigate the mechanisms governing the aberrant nuclear localization of β-catenin in myeloid leukemia.
- This study has characterized the first β-catenin interactomes for hematopoietic cells and identified the transcription factor LEF-1 as a driver of nuclear β-catenin localization in myeloid leukemia cells.

Abstract

Canonical Wnt/β-catenin signaling is frequently dysregulated in myeloid leukemias and is implicated in leukemogenesis. Nuclear-localized β-catenin is indicative of active Wnt signaling and is frequently observed in acute myeloid leukemia patients; however, some patients exhibit little or no nuclear β-catenin even where cytosolic β-catenin is abundant. Control of the subcellular localization of β-catenin therefore represents an additional mechanism regulating Wnt signaling in hematopoietic cells. To investigate the factors mediating the nuclear-localization of β-catenin we carried out the first nuclear/cytoplasmic proteomic analysis of the β-catenin interactome in myeloid leukemia cells and identified putative novel β-catenin interactors. Comparison of interacting factors between Wnt-responsive cells (high nuclear β-catenin) versus Wnt-unresponsive cells (low nuclear β-catenin) suggested the transcriptional partner, LEF-1, could direct the nuclear-localization of β-catenin. The relative levels of nuclear LEF-1 and β-catenin were tightly correlated in both cell lines and in primary AML blasts. Furthermore, LEF-1 knockdown perturbed β-catenin nuclear-localization and transcriptional activation in Wnt-responsive cells. Conversely, LEF-1 overexpression was able to promote both nuclear-localization and β-catenin-dependent transcriptional responses in previously Wnt-unresponsive cells. This is the first β-catenin interactome study in hematopoietic cells and reveals LEF-1 as a mediator of nuclear β-catenin level human myeloid leukemia.

Key words: β-Catenin; Wnt Signaling; LEF-1; Myeloid; Leukemia; Interactome.

Introduction

Canonical Wnt signaling is an evolutionary conserved signal transduction pathway strictly controlled during normal development but frequently dysregulated in cancer.[1] In the absence of a Wnt ligand, the central mediator of this signaling pathway, β-catenin, is constitutively phosphorylated by a destruction complex (DC) consisting of GSK3β, CK1, Axin and APC, priming it for subsequent degradation by the proteasome. Upon Wnt ligand binding to the Wnt receptors (Frizzled and LRP5/6), the DC becomes saturated with phosphorylated β-catenin (which cannot be degraded) resulting in cytosolic accumulation of non-phosphorylated β-catenin.[2] Following nuclear translocation, β-catenin complexes with the T-cell factor (TCF)/lymphoid enhancer factor (LEF) transcriptional regulators and promotes activation of proto-oncogenic Wnt target genes like *c-myc*, *cyclinD1* and *survivin* (http://web.stanford.edu/group/nusselab/cgi-bin/wnt/target_genes). Thus, Wnt signaling activation is dependent on the movement of β-catenin into the nucleus, yet this remains a poorly understood process in blood cells. β-Catenin lacks canonical nuclear-localization or -export sequences and its subcellular distribution has instead been associated with multiple factors in context-dependent settings.[3]

β-Catenin is frequently overexpressed in acute myeloid leukemia (AML)[4] where its expression correlates with inferior patient survival.[5] β-Catenin has been shown to play a key role in the initiation of AML and chronic myeloid leukemia (CML).[6,7] Furthermore, frequent chromosomal aberrations driving AML and CML are known to cooperate with β-catenin.[8,9] Key to the activation of Wnt signaling is the movement of β-catenin into the nucleus and this is frequently observed in AML.[10] We have previously demonstrated that around 10% of primary AML patient blast samples exhibit little nuclear β-catenin expression, despite substantial cytosolic levels, a phenomenon replicated in 10-20% of myeloid leukemia cell lines upon Wnt stimulation.[3,11] In fact, this is characteristic of normal human hematopoietic stem/progenitor cells (HSPC) which similarly limit β-catenin nuclear-localization possibly to protect normal HSC from detrimental levels of Wnt signaling.[12] The

permissive nuclear-localization of β-catenin observed in myeloid leukemias is therefore aberrant and warrants further investigation.

To better understand β-catenin nuclear-localization mechanisms in myeloid leukemia cells, we generated the first β-catenin interactomes in hematopoietic cells. These analyses have shown that LEF-1, a β-catenin-dependent transcription factor, can also regulate the level of nuclear β-catenin in myeloid leukemia cells. The relative level of nuclear LEF-1 expression correlates with relative nuclear levels of β-catenin in primary AML patient blasts indicating this axis has clinical relevance. Furthermore, the nuclear-localization of β-catenin can be promoted by LEF-1 overexpression and conversely is reduced by LEF-1 knockdown. Finally, we demonstrate LEF-1 expression is suppressed in Wnt-unresponsive cells through rapid proteolytic degradation that is not observed in Wnt-responsive cells. Overall, this study characterizes β-catenin interactions within a hematopoietic context and identifies LEF-1 as a regulator of nuclear β-catenin localization in human leukemia.

Methods

Patient samples, cell culture and β-catenin stabilization
Bone marrow, peripheral blood or leukapheresis samples from patients diagnosed with AML/MDS (Clinical information in Supplementary Table S1) were collected in accordance with the Declaration of Helsinki and with approval of University Hospitals Bristol NHS Trust and London Brent Research Ethics Committee. Mononuclear cells were separated using Ficoll-Hypaque (Sigma-Aldrich, Poole, UK) and samples with ≥80% viability included in the study. K562, HEL, ML-1, U937, THP1 and PLB-985 cell lines (ECACC, Salisbury, UK) were cultured as previously described.[11] For proliferation assays cell lines were seeded in triplicate at 1×10^5/ml into 24-well plates within medium containing 10, 5, 1 or 0.5% fetal bovine serum (Labtech, East Sussex, UK) and cellular density counted using a hemocytometer at 24, 48 and 72 hours. For Wnt signaling activation, cell lines were treated with 5μM of the GSK-3β inhibitor CHIR99021 (Sigma-Aldrich) or 1μg/ml recombinant murine Wnt3a (Peprotech, London, UK) for 16hr (unless otherwise stated) at 37°C.

Nuclear/Cytoplasmic fractionation

$2\text{-}8\times10^6$ cells were washed in PBS and resuspended in 250μl cytoplasmic lysis buffer (10mM Tris-HCl (pH8), 10mM NaCl, 1.5mM $MgCl_2$, 0.5% Igepal-CA630/NP40) containing complete™ Mini Protease-Inhibitor Cocktail (PIC; Sigma-Aldrich) for 10min at 4°C. The supernatant (cytosolic fraction) was recovered following centrifugation at 800*g* for 5min, and the nuclear pellet washed twice with PBS. Nuclear pellets were resuspended in lysis buffer (Cell Signaling Technology, Leiden, Netherlands) containing PIC and incubated for 45min with sonication to maximize nuclear lysis. Insoluble material was removed at 21,000*g* for 10min and solubilized nuclear fractions stored at -80°C.

Lentiviral transduction

K562 and HEL cells were lentivirally-transduced with the β-catenin-activated reporter (BAR) or mutant 'found unresponsive' control (fuBAR) system as previously.[11] For LEF-1 knockdown/overexpression, cells were lentivirally-transduced with human LEF-1 shRNA (TRCN0000-020163, -413476, -418104, -428178 and -428355, MISSION® Sigma), or LEF-1 overexpression vector (pLV-EGFP:T2A:Puro-EF1A>hLEF-1 VectorBuilder, Neu-Isenburg, Germany). Cells transduced with scrambled shRNA/empty vector served as controls.

β-catenin co-immunoprecipitation and immunoblotting

For co-immunoprecipitation (co-IP), 8μg of crosslinked β-catenin (Clone-14) or IgG (Clone MOPC-31C) antibody (Becton Dickinson, Oxford, UK) were incubated with 1mg of either pre-cleared cytoplasmic, or nuclear lysate, overnight at 4°C (Supplementary Methods). Subsequently beads were washed x5 prior to proteomic analyses or boiled for 95°C for 5min following washes for immunoblotting. Immunoblotting was performed as previously[13] using antibodies to total β-Catenin (as above), phosphorylated β-catenin (Ser33/37/Thr41), α-Catenin (Clone-5), E-Cadherin (Clone-36), GSK3β (Clone-7; BD), α-tubulin (DM1A), lamin A/C (4C11; Sigma), Axin1 (C76H11), Axin2 (76G6), TCF-4 (C48H11), LEF-1 (C12A5), Survivin (71G4B7), CyclinD1 (92G2; Cell Signaling Technology), active β-catenin (8E7, Merck-Millipore, Watford, UK) and c-MYC (9E10; Santa Cruz, Heidelberg, Germany). β-Catenin and LEF-1 densitometry were performed as described in Supplementary Methods.

Mass spectrometry (MS) and data analyses

Cytosolic or nuclear β-Catenin/IgG co-IP's were prepared and analyzed by MS as detailed in Supplementary Methods. Post-acquisition, duplicate values and proteins detected by only a single peptide were first removed. Tandem Mass Tag (TMT) ratios were imported into Perseus v1.5.6.0 (Max Planck Institute of Biochemistry, Munich, Germany) followed by logarithmic transformation, normalization (through median subtraction) and removal of proteins not present in at least 2 of 3 replicates. A one-sample *t* test was performed with significance of protein binding (-Log$_{10}$ *p* value) plotted versus fold change in protein binding (Log$_2$). The MS proteomics data have been deposited to the ProteomeXchange Consortium (http://proteomecentral.proteomexchange.org) via the PRIDE partner repository with the dataset identifier PXD009305. Interaction specificity was assessed using the publicly available CRAPome database (Contaminant Repository for Affinity Purification: http://www.crapome.org).

Assessment of TCF reporter and flow cytometry

Activity of BAR lentiviral construct was performed as previously.[11] Multi-parameter flow cytometric measurements were acquired using a MACSQuant® Analyzer 10 in conjunction with MACSQuantify™ v2.8 (Miltenyi Biotec, Bisley, UK) or an Accuri C6 in conjunction with C sampler software v1.0.264.21 (BD). Post-acquisition analyses were performed using FlowJo v10.5.3 (Tree Star Inc, Ashland, OR). Threshold for TCF reporter fluorescence was set using matched-controls expressing mutant 'found unresponsive' fuBAR. Cell viability was assessed using 2μg/mL propidium iodide (Miltenyi Biotech).

Statistics

Statistical analyses were performed using GraphPad Prism v7.0 (GraphPad Software Inc., San Diego, CA) and Perseus. Correlation was assessed using a Spearman's Rank correlation coefficient (R). Significance of difference was assessed using a one-sample or Students' *t* test and data represents mean±1 SD derived from three biological replicates.

Results

Myeloid leukemia cell lines exhibit heterogeneous nuclear β-catenin localization and Wnt activation

Previously we showed that myeloid leukemia cell lines vary markedly in their capacity for nuclear β-catenin localization upon Wnt stimulation, mimicking the heterogeneity of nuclear β-catenin translocation in AML patients.[11] To investigate the mechanistic basis for this, we selected two sets of myeloid leukemia lines which differed markedly in Wnt signaling output in response to agonist. K562 and HEL were Wnt-responsive cell lines that localized high levels of β-catenin into the nucleus upon treatment with the Wnt agonist, CHIR99021, a GSK3β inhibitor (Figure 1A). Cell viability was not significantly affected by 16hr CHIR99021 treatment (Supplementary Figure S1AB). Similar patterns of subcellular localization were observed for the active (non-phosphorylated) form of β-catenin in response to CHIR99021 (Supplementary Figure S1C). As expected, the phosphorylated forms of β-catenin (Ser33/37/Thr41) were reduced upon CHIR99021 treatment (Supplementary Figure S1C). Correspondingly these lines showed robust induction of a TCF reporter (a measure of β-catenin-dependent transcription), whilst cells expressing reporter with a mutated TCF binding site showed no induction (Figure 1B). In contrast, ML-1 and U937 cells had a highly restricted capacity for nuclear β-catenin localization (versus K562 and HEL cells) despite substantial cytosolic stabilization of the protein (Figure 1B and C). Consistent with this, CHIR99021 treatment of ML-1 or U937 cells caused no detectable activation of the TCF reporter (Figure 1B and 1D). The same patterns of Wnt-responsiveness were observed when cell lines were treated with rWnt3a (Supplementary Figure S2). These findings demonstrate that the ability of some leukemia cells to drive a transcriptional response to Wnt agonist is limited by their capacity to permit the nuclear accumulation of β-catenin and we termed these cells Wnt-unresponsive.

β-Catenin interactome analyses reveal contrasting protein interactions between Wnt-responsive and Wnt-unresponsive leukemia cell lines

Given the wealth of factors previously reported to regulate the nuclear localization of β-catenin,[3] we designed an interactome screen of cytosolic and nuclear β-catenin interacting partners from representative Wnt-responsive (K562 and HEL), and Wnt-

unresponsive (ML1) cell lines so that we could shortlist candidate factors involved in this process (Figure 2A). Prior to mass spectrometry, we validated the efficiency of β-catenin co-immunoprecipitation (co-IP) (Figure 2B) from both a positive control for high β-catenin expression (SW620 colorectal cells containing mutated APC: demonstrating a 4.0- and 4.3-fold enrichment of β-catenin in cytosol and nuclear fractions respectively) and in the context of agonist-stabilized β-catenin (HEL: showing a 6.3- and 9.1-fold enrichment). We also confirmed co-IP of a known interactor; TCF-4 (*TCF7L2*) from the nuclear compartment.

Following mass spectrometry, raw tandem mass tag (TMT) ratios were processed to generate a set of statistically ranked interactions based on significance of fold-change in protein binding (raw and processed MS data available in Supplementary MS Data Excel sheets). An extensive profile of β-catenin interactions were observed in K562 cells (225 significantly enriched cytosolic interactions, 118 significantly enriched nuclear interactions; Figure 3A and 3B). In contrast, a comparatively sparse interaction profile was observed in ML1 cells (38 significantly enriched cytosolic interactions, 26 significantly enriched nuclear interactions; Figure 3C and 3D). An extensive repertoire of β-catenin interactions was also detected in the other Wnt-responsive cell line analyzed, (HEL; 154 significantly enriched cytosolic interactions, 138 significantly enriched nuclear interactions; Supplementary Figure S3). The sparse nuclear β-catenin interaction network observed in ML1 cells is perhaps unsurprising given the low levels of nuclear β-catenin, however the relative paucity of interactors observed in the cytosol of this line was more surprising given the comparable abundance of β-catenin in this fraction compared with K562/HEL cells.

Our experimental and bioinformatics strategy was validated by the identification of known β-catenin interactions (highlighted in green), which were also more abundant in the K562 cells (23 in cytosol, 26 in nucleus) versus the ML-1 cells (7 in cytosol, 8 in nucleus). From our significantly enriched interactions (red dots; Figure 3 panels), we identified several putative novel partners for β-catenin as summarized for K562 (Figure 4A, B and Supplementary Table S2), ML1 (Figure 4C, D and Supplementary Table S2), and for HEL (Supplementary Figure S4 and Supplementary Table S3). Within these significant interactions we identified a number of novel associations of particular interest to myeloid leukemias and/or Wnt signaling which appeared in one

or more cell lines (red asterisks), but were outside the remit of this study to investigate further. MBD3 and PRC1 have been found to cooperate with the oncogenic fusion proteins PML/RARα[14] or PLZF/RARα[15] in acute promyelocytic leukemia (APL), and regulate stemness through Wnt/β-catenin signaling.[16,17] The RNA binding protein MSI2 predicts poor prognosis in AML,[18] more aggressive CML,[19] and can promote cancer via Wnt signaling.[20] LIN28B, a microRNA-binding protein, is overexpressed in multiple leukemias including AML,[21] where it promotes proliferation,[22] and cooperates with Wnt signalling to drive malignancy.[23] DDX10, RBM6 and RBM15 are known to form oncogenic fusion proteins in myeloid leukemias,[24-26] and DDX10 and RBM15 also have roles in promoting Wnt signaling.[27,28] PUM2 and MKRN2 are two further proteins reported to promote the growth of both normal and malignant hematopoietic cells.[29,30] We also confirmed the first reported β-catenin interaction with Wilms Tumour-1 (WT1) by MS and immunoblotting (Supplementary Figure S5), which is of considerable interest in leukemia biology given its frequent dysregulation in AML and association with adverse patient survival.[31]

Nuclear LEF-1 expression correlates with nuclear β-catenin localization in cell lines and primary AML patient cells

We next examined the data from the fractions of Wnt-responsive cells for candidate proteins that could promote the nuclear-localization of β-catenin. Several had previously been implicated in negative regulation of β-catenin nuclear localization: GSK3β,[32] α-catenin,[33] Axin1/2,[34] and APC[34]; whilst TCF-4[34] and LEF-1[35] are nuclear localized transcription factors that bind β-catenin. To validate the MS data, we examined the protein expression of these candidates in a panel of myeloid cell lines by immunoblotting. With the exception of APC (which is problematic to blot)[36] immunoblotting confirmed MS analysis in that expression of the negative regulators was mostly limited to Wnt-responsive cells making it unlikely they were responsible for restricted nuclear β-catenin in Wnt-unresponsive cells (Figure 5A).

We next examined the expression of two known nuclear β-catenin interactors, TCF-4 and LEF-1, which are ubiquitously expressed in multiple tissues. Both of these proteins are predominantly nuclear in Wnt-responsive cell lines and were absent from the Wnt-unresponsive lines (Figure 5A; matching the proteomics data in Figure

3 and also Supplementary Figure S3). Of these two proteins, LEF-1 bound β-catenin with higher significance than TCF4 in both K562 and HEL nuclei. This, together with our previous observation that overexpression of TCF-4 actually suppressed β-catenin-dependent transcription[37] (and thus is unlikely to promote nuclear β-catenin level) led us to focus our investigation on LEF-1. This protein is known to be dysregulated in AML[38] so we examined the clinical relevance of this by correlating relative LEF-1 nuclear localization with that of β-catenin in primary AML blasts. In our cohort of 23 nuclear/cytosol fractionated AML patient samples we observed a highly significant degree of correlation (Spearman Rank R=0.63, *P*<0.005) between the relative nuclear-localized (as a proportion of total) β-catenin protein and relative nuclear-localized (as a proportion of total) LEF-1 protein (Figures 5B and C). Interestingly, the overall frequency of β-catenin protein expression observed in this largely pediatric AML cohort was higher than previous reports (Supplemental Figure S6). Taken together, these data indicate that nuclear β-catenin translocation capacity is linked to LEF-1 expression in myeloid cell lines, and nuclear LEF-1 is a strong clinical predictor of nuclear β-catenin levels in patient-derived AML blasts.

Modulation of LEF-1 expression in myeloid cells regulates nuclear-localization of β-catenin and alters Wnt-responsiveness.

The above data indicated a correlative relationship between nuclear LEF-1 level and capacity for nuclear β-catenin localization. To demonstrate causation, we examined the effect of modulating LEF-1 expression on β-catenin localization. Initially, we tested multiple *LEF1* shRNA sequences (Supplementary Figure S7A) and selected the most optimal (TRCN0000428355) for knockdown of nuclear LEF-1 expression in the Wnt-responsive K562 and HEL cell lines. This approach resulted in a 72%±7% knockdown in LEF-1 protein in the nuclei of K562 cells and an 89%±4% knockdown in HEL cells (Figure 6A). Somewhat lower levels of LEF-1 knockdown were observed in CHIR99021-treated cells (65%±19% and 83%±7%, respectively) probably a result of *LEF1* being a Wnt target gene and thus being induced through Wnt agonist treatment.[39] LEF-1 knockdown perturbed nuclear localization of β-catenin by approximately a third (28%) in K562 following CHIR99021 treatment, proportionate to control cells. This reduction was accentuated in HEL cells (41%) which corresponded to the greater degree of LEF-1 knockdown in these cells (Figure 6B).

The knockdown of LEF-1 protein resulted in significantly reduced growth of both K562 and HEL cells at multiple timepoints across a range of serum concentrations (Figure 6C). Use of a second *LEF1* shRNA and a different method of Wnt stimulation (rWnt3a) resulted in a similar finding (Supplementary Figure S7B and C). These data suggest LEF-1 promotes the optimal translocation of β-catenin into the nucleus of Wnt-responsive cells and contributes partly to their growth.

Next, we examined whether LEF-1 expression was sufficient to permit nuclear-localization of β-catenin. To establish this, we stably overexpressed *LEF1* in the Wnt-unresponsive (and LEF-1 negative) U937 and ML1 cells. Overexpression of LEF-1 resulted in substantial cytosolic expression of the full-length LEF-1 protein (50kDa) but weak nuclear expression; despite this we observed a dramatic increase in nuclear localized β-catenin in both ML1 (4-fold) and U937 (2.3-fold) cells overexpressing *LEF1* following CHIR99021 treatment (Figure 6D and E). This disparity may be explained by the abundant expression of a short-form of LEF-1 in the nucleus (25-30kDa) that was absent in Wnt-responsive lines (discussed below). These effects were mirrored using Wnt3a treatment (Supplementary Figure S7C) and we also showed that LEF-1 overexpression was able to facilitate nuclear localization of β-catenin in two further AML cell lines (PLB-985 and THP1; Supplementary Figure S7D). These data demonstrate that overexpression of LEF-1 can significantly increase the capacity for nuclear β-catenin localization in Wnt-unresponsive cell lines.

To assess the impact of LEF-1 knockdown (and subsequent nuclear β-catenin reduction) on Wnt signaling, we measured TCF reporter activity. As predicted, Wnt signaling induction in Wnt-responsive K562 and HEL cells following CHIR99021 treatment was severely diminished following LEF-1 knockdown (Figures 7A and B). A significant reduction in Wnt signaling output was also observed following use of an alternative *LEF1* shRNA in response to CHIR99021 or Wnt3a stimulation (Supplementary Figure S8). Assessment of the TCF reporter activity in the *LEF1* overexpressing lines was not possible due to the confounding expression of the GFP selectable marker; instead we examined the protein expression of the classic downstream Wnt target proteins survivin, c-MYC and cyclinD1. We found that *LEF1* overexpression significantly enhanced the expression of these proteins following

CHIR99021 treatment (Figure 7C and D), indicating that the observed translocation of β-catenin was sufficient to generate a transcriptional response. A caveat to these data is that these observations cannot be linked exclusively to the modulation of β-catenin nuclear-localization since LEF-1 expression is a co-variable in these experiments. Taken together, these data indicate LEF-1 can regulate the nuclear level of β-catenin and our observations are also consistent with a concomitant regulation of Wnt signaling activity.

LEF-1 protein is proteolytically cleaved in Wnt-unresponsive cells
In the experiments above, overexpression of full-length LEF-1 in Wnt-unresponsive cell lines resulted in the emergence of a 25-30kDa species of LEF-1 protein. To evaluate the contribution of this short LEF-1 form with the increased nuclear β-catenin level observed in these cell lines we examined the β-catenin binding capacity of this species. We performed β-catenin co-IP from both the cytosol and nucleus of CHIR99021 treated *LEF1*-overexpressing U937 cells and immunoblotted for LEF-1 protein. As observed in Figure 8A, both the full-length and short-forms of LEF-1 protein co-IP'd with β-catenin from the cytosol implying both forms bind β-catenin in this cell line. In the nuclear fraction, β-catenin preferentially co-IP'd with the short LEF-1 form, though the proportion of short-form was highly enriched in this fraction (Figure 8A; input lane). These data confirm that the short-form LEF-1 has β-catenin binding ability and could mediate the increased nuclear β-catenin translocation observed in Wnt-unresponsive cell lines above upon LEF-1 overexpression with CHIR99021 treatment.

Finally, we examined the origin of the short LEF-1 polypeptide. This variant was unlikely derived from alternative splicing since the ectopic expression of LEF-1 was driven from cDNA. Furthermore, these short forms of LEF-1 were also observed endogenously in colorectal cell lines (Supplementary Figure S9A) and in primary AML samples featured in Figure 5 (full blots in Supplementary Figure S9B). Therefore, the presence of short-form LEF-1 was most consistent with a proteolytic cleavage mechanism. To investigate this, nuclear lysates from both K562 control and U937-*LEF1* cells ± protease inhibitor cocktail (PIC) were incubated at 37°C and the relative proportions of full-length to short LEF-1 forms in each cell line observed over 0-60 minutes. In K562 control cells, full-length LEF-1 protein was stable with no

detectable breakdown of full-length LEF-1 protein even in the absence of PIC (Figure 8B). In contrast, the full-length LEF-1 band present in U937-LEF-1 cells was reduced with concomitant enrichment of the short-form polypeptide after a 10 min incubation at 37°C (Figure 8C). The removal of the PIC reduced the half-life of full-length LEF-1 by approximately 50% with degradation occurring within 5 min. Together these data are consistent with the short-form of LEF-1 arising through proteolytic processing. These data suggest that LEF-1-targeted proteases are active in Wnt-unresponsive U937 cells, but inactive/absent in Wnt-responsive K562 cells. To test this, we mixed nuclear lysates from K562 cells directly with whole cell lysates from U937 control cells (which are LEF-1 negative). Remarkably, the previously stable full-length LEF-1 band present in K562 cells exhibited marked and rapid reduction with a concomitant increase in the short-form polypeptide, a process exacerbated by PIC removal (Figure 8D). These data confirm that constitutive LEF-1 degradation mechanisms are active in Wnt-unresponsive cells but are absent/inhibited in Wnt-responsive cells.

Discussion

Canonical Wnt signaling has emerged as one of the most frequently dysregulated signaling pathways in myeloid neoplasms which has led to considerable interest in targeting this pathway. The central mediator β-catenin represents an appealing therapeutic target because of its leukemogenic role,[6,7] prognostic influence[5] and functional redundancy in normal hematopoietic development.[40] The characterization of β-catenin's hematopoietic interactome is therefore of considerable interest and the experimental approach adopted in this study was validated by the identification of multiple known β-catenin partners such as Axin, TCF-4, α-catenin and APC. Associations with key hematopoietic transcription factors, C/EBPζ and GATA-1, were identified and these are known to co-occupy genomic sites with TCF-4 (a known β-catenin partner) during hematopoietic development.[41] We confirmed the previously reported interaction of β-catenin with the oncogenic fusion protein BCR-ABL in CML, which is present in K562 cells.[9] In addition to known partners, we identified putative novel interactions which have known relevance to leukemia and/or Wnt signaling (MBD3,[14,16] PRC1,[15,17] MSI2,[18-20] LIN28B,[21-23] DDX10,[24,27] RBM6,[25] RBM15,[26,28] PUM2,[29] MKRN2[30] and WT1[31]).

For investigating β-catenin nuclear localization mechanisms we focused on LEF-1 given that it was one of the most significantly enriched interactors present in Wnt-responsive cell nuclei, and its nuclear expression was highly predictive of β-catenin nuclear-localization in both myeloid cell lines and primary AML blasts. A role for LEF-1 in mediating nuclear-localization of β-catenin was confirmed using both knockdown and overexpression approaches. LEF-1 contains a nuclear localization sequence and is known to shuttle between cytoplasmic and nuclear compartments.[42] This suggests LEF-1 could serve as a cytosolic-nuclear chaperone for β-catenin, however the high nuclear:cytosol ratio of LEF-1 expression observed in Wnt-responsive cells (K562 and HEL) would be more consistent with LEF-1 serving as a nuclear retention factor for β-catenin, as has been demonstrated previously for other Wnt signaling components.[34] This is the first evidence of LEF-1 contributing to β-catenin nuclear-localization capacity in human myeloid leukemia cells, however our data cannot exclude the role of other factors in this process. Nuclear export mechanisms may also be influential in limiting nuclear accumulation of β-catenin in Wnt-unresponsive cell lines. In particular, RanBP1 was an interacting partner detected for β-catenin in ML-1 nuclei but absent in K562/HEL nuclei and may warrant further study given the documented role for RanBP3 in mediating β-catenin export.[43] Two factors recently implicated in nuclear β-catenin regulation including RAPGEF5[44] and Twa1,[45] were not detected in our analyses, suggesting their interaction with β-catenin is context-dependent.

A strong correlation between the relative levels of nuclear localized β-catenin and LEF-1 was identified in primary AML samples suggesting this relationship may have clinical relevance. Indeed, expression of constitutively active LEF-1 in HSPCs induced AML in mice,[38] and LEF-1 expression promotes the survival of myeloid leukemia cell lines.[46] In our study, we observed significantly inhibited growth in K562 and HEL cells harboring LEF-1 knockdown (Figure 6C). Given the adverse prognosis of nuclear β-catenin in AML[5] and recent studies demonstrating its therapeutic merit in AML models,[47-49] LEF-1 represents an attractive target in myeloid leukemia

through also inhibiting β-catenin nuclear localization. Small molecule inhibitors of β-catenin: TCF/LEF interaction are in development and have shown efficacy in leukemia treatment.[50-52] It would be interesting to observe if this efficacy is partly driven by reducing the level of nuclear β-catenin in leukemia cells. This study focused on the role of LEF-1 driving aberrant β-catenin nuclear-localization in myeloid leukemia however, given the frequency of Wnt/β-catenin dysregulation in human cancer, this axis could be active in other malignancies.

We also observed that LEF-1 is proteolytically degraded in Wnt-unresponsive leukemia cells resulting in the emergence of short-form LEF-1 proteins (25-30kDa). These were smaller than the 38kDa transcriptional isoforms previously reported to derive from alternative splicing or alternative promoter usage[39,53] which serve as dominant-negative inhibitors of Wnt signaling because they lack the β-catenin binding domain necessary to initiate transcription.[39] In contrast, the proteolytic fragments observed in this study retained β-catenin binding capacity (Figure 7A) and did not appear to have dominant-negative function (Wnt targets were still activated; Figure 6C and D). Under the conditions of the experiment, however, where LEF-1 is being overexpressed, the abundance of these fragments may have a dominant effect on β-catenin retention in the nucleus, whereas under normal circumstances, it is likely that degradation serves to remove LEF-1 and suppress the nuclear retention of β-catenin. This post-translational regulation of LEF-1 has parallels with embryonic stem cells where proteolytic cleavage of TCF-3 (*TCF7L1*), a closely related family member, removes it from target genes when differentiation signals trigger the suppression of Wnt signaling.[54] In leukemia cells this proteolytic cleavage could be mediated by NLK (Nemo-like kinase) which binds the E3 ubiquitin-ligase NARF (NLK associated RING finger protein) and reportedly induces ubiquitylation (and proteasomal degradation) of LEF-1 in cooperation with the E2 conjugating enzyme E2-25K;[55] a mechanism previously reported to be active in leukemia cells.[56]

In summary, our study has made three key findings; firstly, the generation of the first β-catenin interactomes in leukemia cells; secondly, the characterization of LEF-1 as

a regulator of nuclear β-catenin localization in leukemia and finally, the demonstration of post-transcriptional proteolytic degradation mechanisms for controlling LEF-1 expression in myeloid leukemia cells.

Disclosure of Potential Conflicts of Interest

No conflict of interest declared.

Author contributions

RGM designed and performed experiments, analyzed data and wrote the manuscript. JR, MP and SD performed experiments, KH and MW performed proteomic analyses. AG developed co-IP methodology and provided manuscript advice. ADD, ACW and AB provided technical guidance and manuscript advice. MW provided experimental advice whilst AT and RLD provided project direction and co-wrote the manuscript.

Acknowledgements

References

1.   Nusse R, Clevers H. Wnt/beta-Catenin Signaling, Disease, and Emerging Therapeutic Modalities. Cell. 2017;169(6):985-999.
2.   Li VS, Ng SS, Boersema PJ, et al. Wnt signaling through inhibition of beta-catenin degradation in an intact Axin1 complex. Cell. 2012;149(6):1245-1256.

3.　　Morgan RG, Ridsdale J, Tonks A, Darley RL. Factors affecting the nuclear localization of beta-catenin in normal and malignant tissue. J Cell Biochem. 2014;115(8):1351-1361.

4.　　Simon M, Grandage VL, Linch DC, Khwaja A. Constitutive activation of the Wnt/beta-catenin signalling pathway in acute myeloid leukaemia. Oncogene. 2005;24(14):2410-2420.

5.　　Ysebaert L, Chicanne G, Demur C, et al. Expression of beta-catenin by acute myeloid leukemia cells predicts enhanced clonogenic capacities and poor prognosis. Leukemia. 2006;20(7):1211-1216.

6.　　Wang Y, Krivtsov AV, Sinha AU, et al. The Wnt/beta-catenin pathway is required for the development of leukemia stem cells in AML. Science. 2010;327(5973):1650-1653.

7.　　Zhao C, Blum J, Chen A, et al. Loss of beta-catenin impairs the renewal of normal and CML stem cells in vivo. Cancer Cell. 2007;12(6):528-541.

8.　　Muller-Tidow C, Steffen B, Cauvet T, et al. Translocation products in acute myeloid leukemia activate the Wnt signaling pathway in hematopoietic cells. Mol Cell Biol. 2004;24(7):2890-2904.

9.　　Coluccia AM, Vacca A, Dunach M, et al. Bcr-Abl stabilizes beta-catenin in chronic myeloid leukemia through its tyrosine phosphorylation. EMBO J. 2007;26(5):1456-1466.

10.　　Griffiths EA, Golding MC, Srivastava P, et al. Pharmacological targeting of beta-catenin in normal karyotype acute myeloid leukemia blasts. Haematologica. 2015;100(2):e49-52.

11.　　Morgan RG, Pearn L, Liddiard K, et al. gamma-Catenin is overexpressed in acute myeloid leukemia and promotes the stabilization and nuclear localization of beta-catenin. Leukemia. 2013;27(2):336-343.

12.　　Luis TC, Ichii M, Brugman MH, Kincade P, Staal FJ. Wnt signaling strength regulates normal hematopoiesis and its deregulation is involved in leukemia development. Leukemia. 2012;26(3):414-421.

13.　　Morgan RG, Mortensson E, Legge DN, et al. LGR5 expression is regulated by EGF in early colorectal adenomas and governs EGFR inhibitor sensitivity. Br J Cancer. 2018;118(4):558-565.

14.　　Morey L, Brenner C, Fazi F, et al. MBD3, a component of the NuRD complex, facilitates chromatin alteration and deposition of epigenetic marks. Mol Cell Biol. 2008;28(19):5912-5923.

15.　　Boukarabila H, Saurin AJ, Batsche E, et al. The PRC1 Polycomb group complex interacts with PLZF/RARA to mediate leukemic transformation. Genes Dev. 2009;23(10):1195-1206.

16.　　Kim JJ, Khalid O, Vo S, Sun HH, Wong DT, Kim Y. A novel regulatory factor recruits the nucleosome remodeling complex to wingless integrated (Wnt) signaling gene promoters in mouse embryonic stem cells. J Biol Chem. 2012;287(49):41103-41117.

17.　　Chiacchiera F, Rossi A, Jammula S, et al. Polycomb Complex PRC1 Preserves Intestinal Stem Cell Identity by Sustaining Wnt/beta-Catenin Transcriptional Activity. Cell Stem Cell. 2016;18(1):91-103.

18.　　Byers RJ, Currie T, Tholouli E, Rodig SJ, Kutok JL. MSI2 protein expression predicts unfavorable outcome in acute myeloid leukemia. Blood. 2011;118(10):2857-2867.

19.　　Kaeda J, Ringel F, Oberender C, et al. Up-regulated MSI2 is associated with more aggressive chronic myeloid leukemia. Leuk Lymphoma. 2015;56(7):2105-2113.

20.   Li Z, Jin H, Mao G, Wu L, Guo Q. Msi2 plays a carcinogenic role in esophageal squamous cell carcinoma via regulation of the Wnt/beta-catenin and Hedgehog signaling pathways. Exp Cell Res. 2017;361(1):170-177.

21.   Helsmoortel HH, De Moerloose B, Pieters T, et al. LIN28B is over-expressed in specific subtypes of pediatric leukemia and regulates lncRNA H19. Haematologica. 2016;101(6):e240-244.

22.   Zhou J, Bi C, Ching YQ, et al. Inhibition of LIN28B impairs leukemia cell growth and metabolism in acute myeloid leukemia. J Hematol Oncol. 2017;10(1):138.

23.   Tu HC, Schwitalla S, Qian Z, et al. LIN28 cooperates with WNT signaling to drive invasive intestinal and colorectal adenocarcinoma in mice and humans. Genes Dev. 2015;29(10):1074-1086.

24.   Yassin ER, Abdul-Nabi AM, Takeda A, Yaseen NR. Effects of the NUP98-DDX10 oncogene on primary human CD34+ cells: role of a conserved helicase motif. Leukemia. 2010;24(5):1001-1011.

25.   Gu TL, Mercher T, Tyner JW, et al. A novel fusion of RBM6 to CSF1R in acute megakaryoblastic leukemia. Blood. 2007;110(1):323-333.

26.   Ma Z, Morris SW, Valentine V, et al. Fusion of two novel genes, RBM15 and MKL1, in the t(1;22)(p13;q13) of acute megakaryoblastic leukemia. Nat Genet. 2001;28(3):220-221.

27.   Wang Y XW, Wei SM, Chen XM, Wei L, Tian RH, Meng Li, Xiao BR, Wu PX, Yu YH. Highly expressed DDX10 promotes hepatocellular carcinoma cell proliferation through Wnt/β-catenin signaling. Int J Clin Exp Pathol. 2017;10(5):6047-6053.

28.   Niu C, Zhang J, Breslin P, Onciu M, Ma Z, Morris SW. c-Myc is a target of RNA-binding motif protein 15 in the regulation of adult hematopoietic stem cell and megakaryocyte development. Blood. 2009;114(10):2087-2096.

29.   Naudin C, Hattabi A, Michelet F, et al. PUMILIO/FOXP1 signaling drives expansion of hematopoietic stem/progenitor and leukemia cells. Blood. 2017;129(18):2493-2506.

30.   Lee KY, Chan KY, Tsang KS, et al. Ubiquitous expression of MAKORIN-2 in normal and malignant hematopoietic cells and its growth promoting activity. PLoS One. 2014;9(3):e92706.

31.   Yang L, Han Y, Suarez Saiz F, Minden MD. A tumor suppressor and oncogene: the WT1 story. Leukemia. 2007;21(5):868-876.

32.   Jamieson C, Sharma M, Henderson BR. Regulation of beta-catenin nuclear dynamics by GSK-3beta involves a LEF-1 positive feedback loop. Traffic. 2011;12(8):983-999.

33.   Simcha I, Shtutman M, Salomon D, et al. Differential nuclear translocation and transactivation potential of beta-catenin and plakoglobin. J Cell Biol. 1998;141(6):1433-1448.

34.   Krieghoff E, Behrens J, Mayr B. Nucleo-cytoplasmic distribution of beta-catenin is regulated by retention. J Cell Sci. 2006;119(Pt 7):1453-1463.

35.   Behrens J, von Kries JP, Kuhl M, et al. Functional interaction of beta-catenin with the transcription factor LEF-1. Nature. 1996;382(6592):638-642.

36.   Davies ML, Roberts GT, Stuart N, Wakeman JA. Analysis of a panel of antibodies to APC reveals consistent activity towards an unidentified protein. Br J Cancer. 2007;97(3):384-390.

37.   Daud SS. The Role of WNT Transcription Factor TCF7L2 in Acute Myeloid Leukaemia. Cardiff University. 2014.

38.   Petropoulos K, Arseni N, Schessl C, et al. A novel role for Lef-1, a central transcription mediator of Wnt signaling, in leukemogenesis. J Exp Med. 2008;205(3):515-522.

39.   Hovanes K, Li TW, Munguia JE, et al. Beta-catenin-sensitive isoforms of lymphoid enhancer factor-1 are selectively expressed in colon cancer. Nat Genet. 2001;28(1):53-57.

40.   Koch U, Wilson A, Cobas M, Kemler R, Macdonald HR, Radtke F. Simultaneous loss of beta- and gamma-catenin does not perturb hematopoiesis or lymphopoiesis. Blood. 2008;111(1):160-164.

41.   Trompouki E, Bowman TV, Lawton LN, et al. Lineage regulators direct BMP and Wnt pathways to cell-specific programs during differentiation and regeneration. Cell. 2011;147(3):577-589.

42.   Prieve MG, Guttridge KL, Munguia JE, Waterman ML. The nuclear localization signal of lymphoid enhancer factor-1 is recognized by two differentially expressed Srp1-nuclear localization sequence receptor proteins. J Biol Chem. 1996;271(13):7654-7658.

43.   Hendriksen J, Fagotto F, van d, V, van SM, Noordermeer J, Fornerod M. RanBP3 enhances nuclear export of active (beta)-catenin independently of CRM1. J Cell Biol. 2005;171(5):785-797.

44.   Griffin JN, Del Viso F, Duncan AR, et al. RAPGEF5 Regulates Nuclear Translocation of beta-Catenin. Dev Cell. 2018;44(2):248-260.e4.

45.   Lu Y, Xie S, Zhang W, et al. Twa1/Gid8 is a beta-catenin nuclear retention factor in Wnt signaling and colorectal tumorigenesis. Cell Res. 2017;27(12):1422-1440.

46.   Skokowa J, Cario G, Uenalan M, et al. LEF-1 is crucial for neutrophil granulocytopoiesis and its expression is severely reduced in congenital neutropenia. Nat Med. 2006;12(10):1191-1197.

47.   Stoddart A, Wang J, Hu C, et al. Inhibition of WNT signaling in the bone marrow niche prevents the development of MDS in the Apc(del/+) MDS mouse model. Blood. 2017;129(22):2959-2970.

48.   Li L, Sheng Y, Li W, et al. beta-Catenin Is a Candidate Therapeutic Target for Myeloid Neoplasms with del(5q). Cancer Res. 2017;77(15):4116-4126.

49.   Jiang X, Mak PY, Mu H, et al. Disruption of Wnt/beta-Catenin Exerts Antileukemia Activity and Synergizes with FLT3 Inhibition in FLT3-Mutant Acute Myeloid Leukemia. Clin Cancer Res. 2018;24(10):2417-2429.

50.   Dandekar S, Romanos-Sirakis E, Pais F, et al. Wnt inhibition leads to improved chemosensitivity in paediatric acute lymphoblastic leukaemia. Br J Haematol. 2014;167(1):87-99.

51.   Minke KS, Staib P, Puetter A, et al. Small molecule inhibitors of WNT signaling effectively induce apoptosis in acute myeloid leukemia cells. Eur J Haematol. 2009;82(3):165-175.

52.   Gandhirajan RK, Staib PA, Minke K, et al. Small molecule inhibitors of Wnt/beta-catenin/lef-1 signaling induces apoptosis in chronic lymphocytic leukemia cells in vitro and in vivo. Neoplasia. 2010;12(4):326-335.

53.   Hovanes K, Li TW, Waterman ML. The human LEF-1 gene contains a promoter preferentially active in lymphocytes and encodes multiple isoforms derived from alternative splicing. Nucleic Acids Res. 2000;28(9):1994-2003.

54.   Shy BR, Wu CI, Khramtsova GF, et al. Regulation of Tcf7l1 DNA binding and protein stability as principal mechanisms of Wnt/beta-catenin signaling. Cell Rep. 2013;4(1):1-9.

55.   Yamada M, Ohnishi J, Ohkawara B, et al. NARF, an nemo-like kinase (NLK)-associated ring finger protein regulates the ubiquitylation and degradation of T cell factor/lymphoid enhancer factor (TCF/LEF). J Biol Chem. 2006;281(30):20749-20760.

56.   Gupta K, Kuznetsova I, Klimenkova O, et al. Bortezomib inhibits STAT5-dependent degradation of LEF-1, inducing granulocytic differentiation in congenital neutropenia CD34(+) cells. Blood. 2014;123(16):2550-2561.

Figure Legends

Figure 1. Myeloid leukemia cell lines exhibit a heterogeneous response to Wnt stimulation. (**A**) Representative immunoblots showing total β-catenin subcellular-localization in myeloid cells following CHIR99021 treatment (GSK3β inhibitor). Lamin A/C and α-tubulin indicate the purity/loading of the nuclear (N) and cytosol (C) fractions respectively. (**B**) Representative flow cytometric histograms showing intensity of the TCF-dependent expression of YFP from the 'β-catenin activated reporter' (BAR) reporter, or negative control 'found unresponsive β-catenin activated reporter' (fuBAR) control (containing mutated promoter binding sites) following treatment with CHIR99021/vehicle control (DMSO) as above. (**C**) Summary showing the relative percentage nuclear β-catenin localization (as a proportion of the total) induced in myeloid cell lines upon CHIR99021 treatment. (**D**) Summary showing the median fluorescence intensity generated from the BAR/fuBAR reporters in myeloid cell lines treated ± CHIR99021. Statistical significance is denoted by *P<0.05 and ****P<0.0001, ns=not significant.

Figure 2. Experimental strategy for analysis of β-catenin interaction partners in myeloid leukemia cell lines. (**A**) Wnt-responsive K562/HEL cells and Wnt-unresponsive cells ML-1 cells were treated with CHIR99021 to stabilize β-catenin prior to cytosolic/nuclear fractionation. From these fractions, either an IgG or β-catenin (β-cat) co-IP was performed generating 8 samples which were each TMT labelled with a unique isobaric mass tag. All samples were pooled, fractionated, cleaned and analysed by mass spectrometry. Mass intensities from each tag report the relative peptide abundance in each sample. Quantitative fold-enrichment of β-catenin co-IP was obtained by comparison with fraction-matched IgG co-IP control.

Three biological replicates were performed on each cell line. (**B**) Representative immunoblots showing the efficiency of total β-catenin co-IP performed from the cytosol or nuclear fractions of SW620 cells and HEL cells. Detection of the known interaction partner TCF-4 was used to assess binding partner efficiency. ID= immunodepleted lysate. β-Catenin arrows represent full-length/degradation intermediates; TCF-4 arrows indicate 58/79kDa transcriptional isoforms.

Figure 3. Proteomics analyses reveal contrasting β-catenin interaction profiles between Wnt-responsive and Wnt-unresponsive leukemia cell lines. Scatter plots showing β-catenin protein interactions detected in (**A**) K562 cytosolic, (**B**) K562 nuclear, (**C**) ML1 cytosolic and (**D**) ML1 nuclear fractions. Vertical dashed red line indicates the threshold for 2-fold change in protein binding at $\log_2$ (=1) relative to IgG co-IP. Horizontal red line represents threshold for significant interactions at *p*=0.05 on $\log_{10}$ scale (=1.3). Highlighted red dots indicate statistically significant interactions and green highlighted events/labels indicate known interactions/associations for β-catenin. Remaining black dots represent other proteins detected in the MS analysis; see also Supplementary MS Data Excel sheets. Fold change values less than 0 are not shown because these likely represent contaminants (see Supplementary MS Data Excel sheets).

Figure 4. Mass spectrometric analyses identify putative novel interaction partners for β-catenin in myeloid leukemia cell lines. Bar graphs summarising the average fold change in protein binding (relative to matched IgG co-IP) for novel, significant β-catenin interactions observed in (**A**) K562 cytosolic, (**B**) K562 nuclear, (**C**) ML1 cytosolic, and (**D**) ML1 nuclear fractions. Significant proteins only are shown (red dots in Figure 2 panels) with a frequency on the CRAPome database of ≤10% and known interactions were removed. Red asterisks represent proteins of particular significance to myeloid leukemias and/or Wnt signaling (see results). Proteins are ranked along X-axis according to statistical significance (left = most significant); see also Supplementary Table S2.

Figure 5. Correlation between nuclear LEF-1 and nuclear β-catenin in leukemia cell lines and primary AML samples. (**A**) Representative immunoblot screen of myeloid leukemia cell lines showing the relative cytoplasmic (C) and nuclear (N) abundance of candidate proteins influencing β-catenin nuclear localization detected

by MS. SW620 colorectal cells were used as a positive control. TCF-4 arrows indicate 58/79kDa transcriptional isoforms. (**B**) Representative immunoblots showing the cytosolic and nuclear expression of both LEF-1 and total β-catenin in primary AML patient samples. LEF-1 protein isoforms migrate as bands between 40-55kDa. Lamin A/C and GAPDH or α-tubulin were used to assess fractionation efficiency and equal protein loading. (**C**) Summary scatter plot showing correlation between relative percentage nuclear β-catenin localization and relative percentage nuclear LEF-1 localization in primary AML patient blasts.

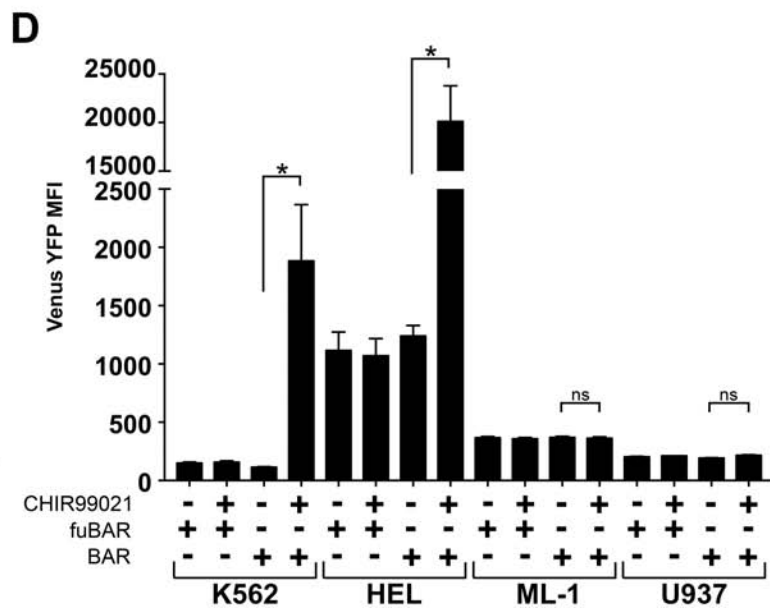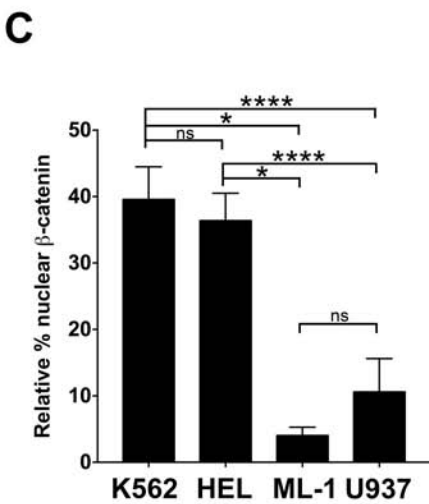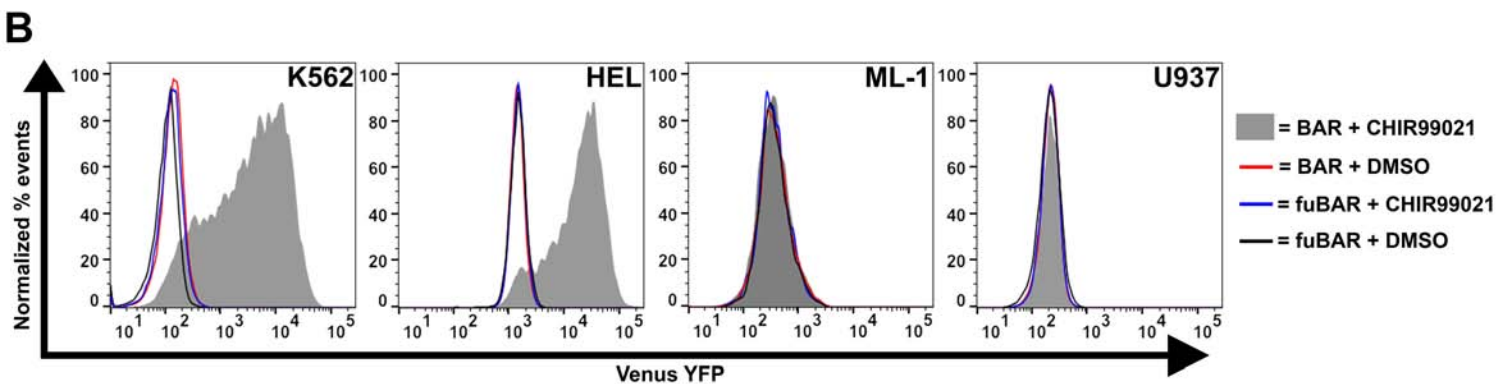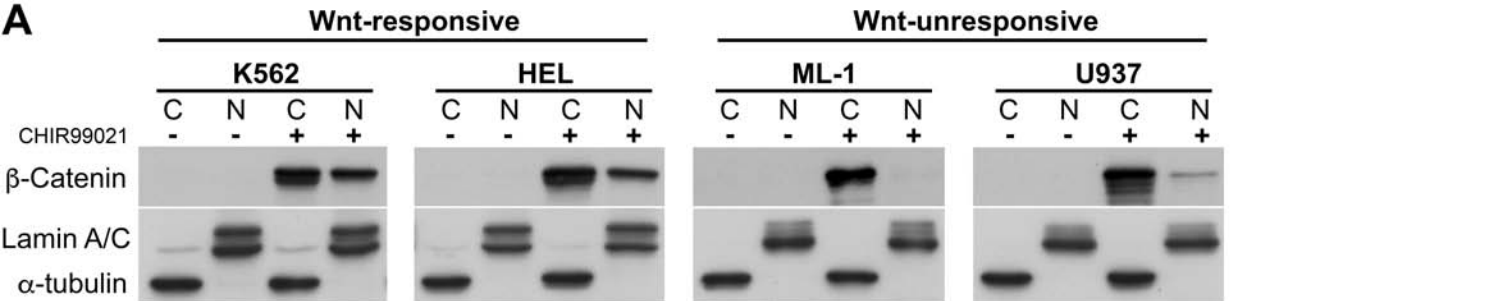**Figure 6. Modulation of LEF-1 expression affects relative nuclear β-catenin level.** (**A**) Representative immunoblots showing the level and subcellular localization of total β-catenin and LEF-1 protein in K562 and HEL cells in response to control/*LEF1* shRNA ± CHIR99021 treatment. Shorter 6hr CHIR99021 treatments were used for these cells to minimise the LEF-1 expression induced through Wnt stimulation. (**B**) Summary graph showing the relative percentage nuclear β-catenin localization induced upon 6hr CHIR99021 treatment of K562 or HEL cells ± control/LEF-1 shRNA. (**C**) Effect of *LEF1* shRNA on the proliferation of K562 and HEL at different concentrations of serum after 24, 48 and 72 hours. (**D**) Representative immunoblots showing the level and subcellular localization of total β-catenin and LEF-1 protein in ML-1 and U937 cells in response to control/*LEF1* overexpression (o/e) ± 16hr CHIR99021 treatment. The positions of full-length (FL) and short-forms (SF) of LEF-1 protein on the blot are indicated by arrows. Lamin A/C and α-tubulin were used to assess fraction purity and protein loading. (**E**) Summary graph showing the relative percentage nuclear β-catenin localization induced upon CHIR99021 treatment of ML-1 and U937 cells for 16hr ± control/*LEF1* overexpression. Statistical significance is denoted by *P<0.05 and **P<0.01.

Figure 7. Modulation of LEF-1 expression affects downstream Wnt signalling. (**A**) Representative flow cytometric histograms showing intensity of the TCF reporter (BAR) in K562 and HEL cells treated with control/*LEF1* shRNA ± CHIR99021. (**B**) Summary data showing the median fluorescence intensity generated from the BAR reporter in K562 and HEL cells treated with control/*LEF1* shRNA ± CHIR99021. (**C**) Representative immunoblots showing expression of known Wnt target proteins survivin, c-MYC and cyclinD1 in ML-1 and U937 cells in response to control/*LEF1*

overexpression ± CHIR99021. Lamin A/C and α-tubulin were used to assess fraction purity and protein loading. (**D**) Summary data showing the relative fold-change in nuclear protein expression of classic Wnt targets survivin, c-MYC and cyclinD1 in CHIR99021 treated ML1 and U937 cells overexpressing *LEF1*. Dashed line represents relative level (=1) present in nuclei of CHIR99021-treated ML1 and U937 cells expressing control plasmid. Statistical significance is denoted by *P<0.05, **P<0.01 and ***P<0.001, ns=not significant.

Figure 8. Short-form LEF-1 is proteolytically-derived and is capable of β-catenin binding. (**A**) Representative immunoblot showing total β-catenin co-IP from cytosolic and nuclear fraction of *LEF1*-overexpressing U937 cells. Total β-Catenin and LEF-1 protein levels are shown. ID= immunodepleted lysate. Representative immunoblot showing LEF-1 protein levels in (**B**) K562 control and (**C**) U937-*LEF1* nuclear lysates ± protease inhibitor cocktail (PIC) during time course incubation at 37°C. (**D**) Representative immunoblots showing LEF-1 protein levels in K562 control nuclear lysate after mixing with U937 control whole cell lysate (1:1 protein concentration) ± PIC during time course incubation at 37°C. Nuclear lamin A/C detection was used to assess protein loading.

A

Wnt-responsive | Wnt-unresponsive

K562 | HEL | ML-1 | U937

CHIR99021: C N C N — — + +

β-Catenin

Lamin A/C

α-tubulin

B

Normalized % events vs Venus YFP

K562, HEL, ML-1, U937

= BAR + CHIR99021
= BAR + DMSO
= fuBAR + CHIR99021
= fuBAR + DMSO

C

Relative % nuclear β-catenin

K562 HEL ML-1 U937

ns, *, ****, *, ****, ns

D

Venus YFP MFI

CHIR99021: − + − + − + − + − + − + − + − +
fuBAR: + + − − + + − − + + − − + + − −
BAR: − − + + − − + + − − + + − − + +

K562 HEL ML-1 U937

A

Wnt-responsive
leukemia cell lines (K562 and HEL, *n*=3)

Wnt-unresponsive
leukemia cell line (ML1, *n*=3)

β-Cat stabilization (CHIR99021 treatment)

β-Cat stabilization (CHIR99021 treatment)

Subcellular fractionation

Subcellular fractionation

Cytosol   Nuclear   Cytosol   Nuclear

IgG Co-IP   β-Cat Co-IP   IgG Co-IP   β-Cat Co-IP   IgG Co-IP   β-Cat Co-IP   IgG Co-IP   β-Cat Co-IP

126   127N   128N   128C   129N   129C   130C   131

Tandem Mass Tag (TMT) peptide labeling (8 isobaric mass tags)

Combine all fractions, fractionate, clean-up, mass spectrometry analysis

Quantitative identification of β-catenin cytoplasmic/nuclear
protein interactions in myeloid leukaemia cells

B

SW620 Cyt   SW620 Nuc   HEL Cyt   HEL Nuc

Input (5%)   IgG ID   β-Cat ID   IgG Co-IP   β-Cat Co-IP

β-Catenin

TCF-4

• = significantly enriched interaction
• = known β-catenin interaction
• = β-catenin bait

A K562 Cyt

B K562 Nuc

C ML1 Cyt

D ML1 Nuc

Significance of protein binding (Log_{10})

Fold change in protein binding (Log_2)

A K562 Cyt

B K562 Nuc

C ML1 Cyt

D ML1 Nuc

A

Wnt-responsive | Wnt-unresponsive

K562 | HEL | U937 | ML1 | SW620

C N | C N | C N | C N | C N

GSK3β
α–Catenin
Axin1
Axin2
→
TCF-4
→
LEF-1
Lamin A/C
GAPDH

B

Primary AML patient blasts

C N C N C N C N | C N C N

β–Catenin
LEF-1
Lamin A/C
α–tubulin

C N C N C N C N | C N C N C N

β–Catenin
LEF-1
Lamin A/C
α–tubulin

C

R=0.63
P<0.005

Relative % nuclear LEF-1

Relative % nuclear β-catenin

A Wnt-responsive

K562 — Cont shRNA / LEF1 shRNA; HEL — Cont shRNA / LEF1 shRNA

CHIR99021: − − + + / − − + +

C N C N / C N C N

β-Catenin, LEF-1, Lamin A/C, α-tubulin

B

Relative % nuclear β-catenin

Cont shRNA / LEF1 shRNA — K562, HEL

C

Cell number (×10⁵/ml) vs % FBS

24hrs, 48hrs, 72hrs — K562 and HEL

● = Cont shRNA
■ = LEF1 shRNA

D Wnt-unresponsive

ML-1 — Cont / LEF1 o/e; U937 — Cont / LEF1 o/e

CHIR99021: − − + + / − − + +

C N C N / C N C N

β-Catenin, LEF-1 (FL, SF), Lamin A/C, α-tubulin

E

Relative % nuclear β-catenin

Cont / LEF1 o/e — ML-1, U937

A U937-*LEF1* Cyt   U937-*LEF1* Nuc

Input (5%), IgG ID, β-Cat ID, IgG Co-IP, β-Cat Co-IP | Input (5%), IgG ID, β-Cat ID, IgG Co-IP, β-Cat Co-IP

β-Catenin

LEF-1

−50
−37
−25

B K562 Control Nuc

PIC + + + + + + − − − − − −
mins @ 37°C 0 2 5 10 30 60 0 2 5 10 30 60

LEF-1

−50
−37
−25

Lamin A/C

C U937-*LEF1* Nuc

PIC + + + + + + − − − − − −
mins @ 37°C 0 2 5 10 30 60 0 2 5 10 30 60

LEF-1

−50
−37
−25

Lamin A/C

D K562 Cont Nuc + U937 Cont whole (1:1)

PIC + + + + + + − − − − − −
mins @ 37°C 0 2 5 10 30 60 0 2 5 10 30 60

LEF-1

−50
−37
−25

Lamin A/C

Supplementary Table S1. Clinical characteristics of AML/MDS patient diagnostic/relapse samples used in this study.

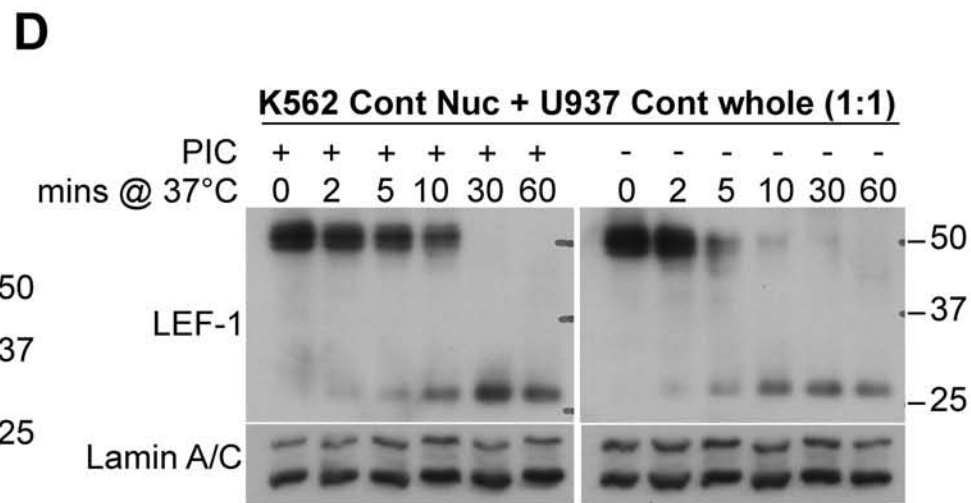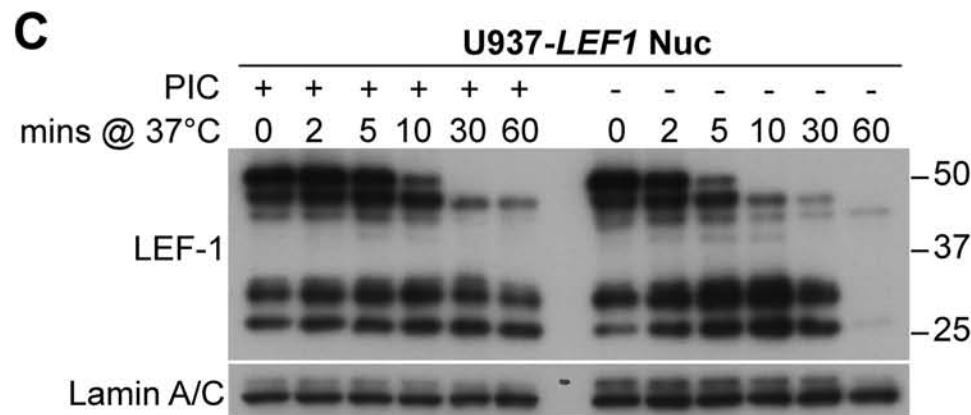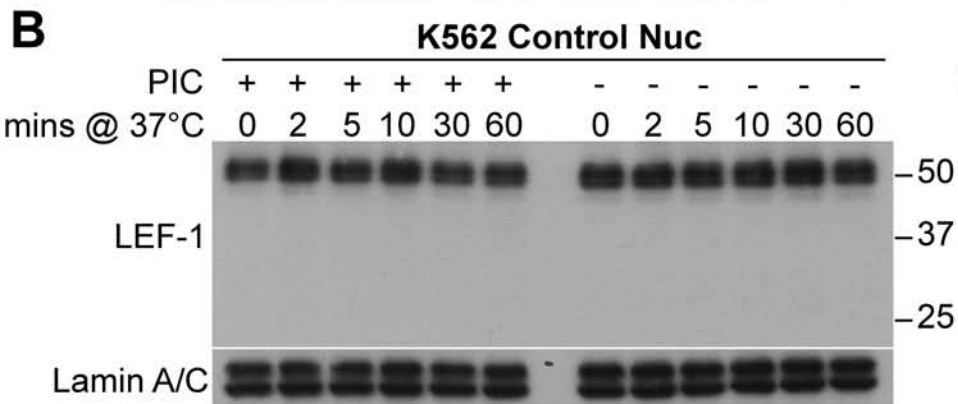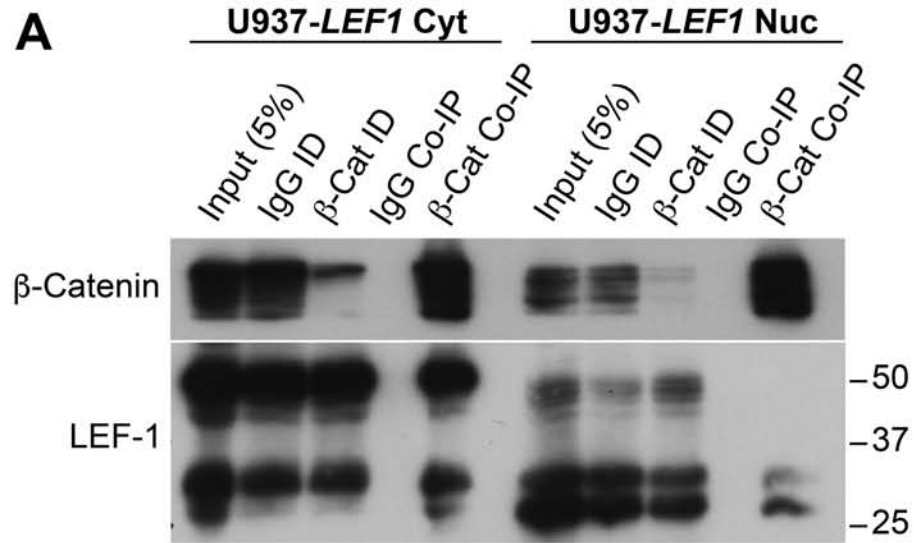| Patient no.	Age (at diagnosis)	Sex	WBC count ($\times 10^9$/L)	Sample type	Secondary disease (Y/N)	Genetic information	Other clinical information
1	76	F	389	LP	N	Normal karyotype, NPM1$^+$, FLT3$^+$	n/a
2	4	M	n/a	BM	n/a	n/a	n/a
3	10	F	n/a	BM	n/a	n/a	Deceased
4	n/a	n/a	>200	PB	Y	n/a	Post-allogeneic transplant. M0/1 (previously diagnosed with M3 10 years previous)
5	6	M	n/a	BM	Y	n/a	Relapse
6	17	M	n/a	BM	Y	n/a	Post-BMT for AML following 2 relapses. Deceased
7	6	M	70.7	n/a	Y	n/a	Secondary to Ewings Sarcoma. Myelomonocytic morphology. Deceased.
8	14	F	7.6	BM	N	MLL rearrangement. Karyotype: 46,XX,ins(10;11)(q11.2;q23.1q23.3).ish ins(10;11)?inv(11)(q23.3)(5'MLL+)(q23.1)(3'MLL+)	BMT for high-risk AML
9	10	M	5.7	BM	N	Monosomy 7 secondary to GATA2 deficiency	BMT for MDS (Barth Syndrome)
10	43	M	16.1	BM	N	Normal karyotype	n/a
11	8	M	4.2	BM	N	t(8;21)(q22;q22) RUNX-RUNX1T1	Phenotype fits WHO criteria of MPAL. MRD negative post treatment course 1 and 2
12	4	M	3.2	BM	N	t(10;11)(p11.2;q23) KMT2A-MLLT10	High risk cytogenetics. BMT.
13	14	F	14.7	PB	N	t(8;21)(q22;q22) RUNX-RUNX1T1	MRD negative post treatment course 1 and 2
14	5	M	1.6	BM	N	n/a	M5. Deceased.
15	2	M	15.0	BM	N	t(8;21)(q22;q22) RUNX-RUNX1T1	n/a
16	8	F	n/a	BM	N	n/a	M4/5. Deceased.
17	7	F	34.4	BM	Y	MLL rearrangement t(9;11)	M5a morphology. BMT following relapse. Deceased
18	n/a	n/a	n/a	LP	n/a	n/a	n/a
19	6	F	20.6	BM	N	Normal karyotype	n/a
20	64	F	13.3	BM	N	Normal karyotype	AML with underlying MDS like changes
21	13	F	91.9	BM	Y	High Risk	Relapsed AML secondary to Rhabdoid tumour. Deceased

22	15	F	6.5	BM	N	MLL (KMT2A) rearrangement, t(10;11)(p11-p14,q23), MLL-MLLT10	MRD detected post treatment course 1
23	4	F	2.6	BM	N	Normal karyotype, NPM1$^+$	MRD neg
24	7	M	3.5	BM	N	t(8;21)(q22;q22) RUNX-RUNX1T1	
25	17	M	n/a	BM	N	t(15;17)(q24;q12)	
26	2	M	2.4	BM	N	t(9;11)(p22;q23), t(11;21)(q23;q8)	
27	14	F	2.1	BM	N	-7	BMT
28	11	M	n/a	BM	N	n/a	BMT for MDS. Deceased
29	7	F	n/a	BM	N	MPAL, 46XX, del5q, abnormal 21	
30	4mo	M	5.1	BM	N	t(9;11)	BMT
31	10	F	1.4	BM	N	n/a	
32	9	M	13.0	BM	N	Pericentric inversion of chromosome 16	90% blasts in BM, 73% blasts in PB
33	6	M	n/a	BM	N	n/a	

BM = Bone marrow
PB = Peripheral blood
LP = Leukapheresis
MRD = Minimal residual disease
BMT = Bone marrow transplant
AML= Acute myeloid leukemia
MDS= Myelodysplastic syndrome
MPAL= Mixed phenotype acute leukemia
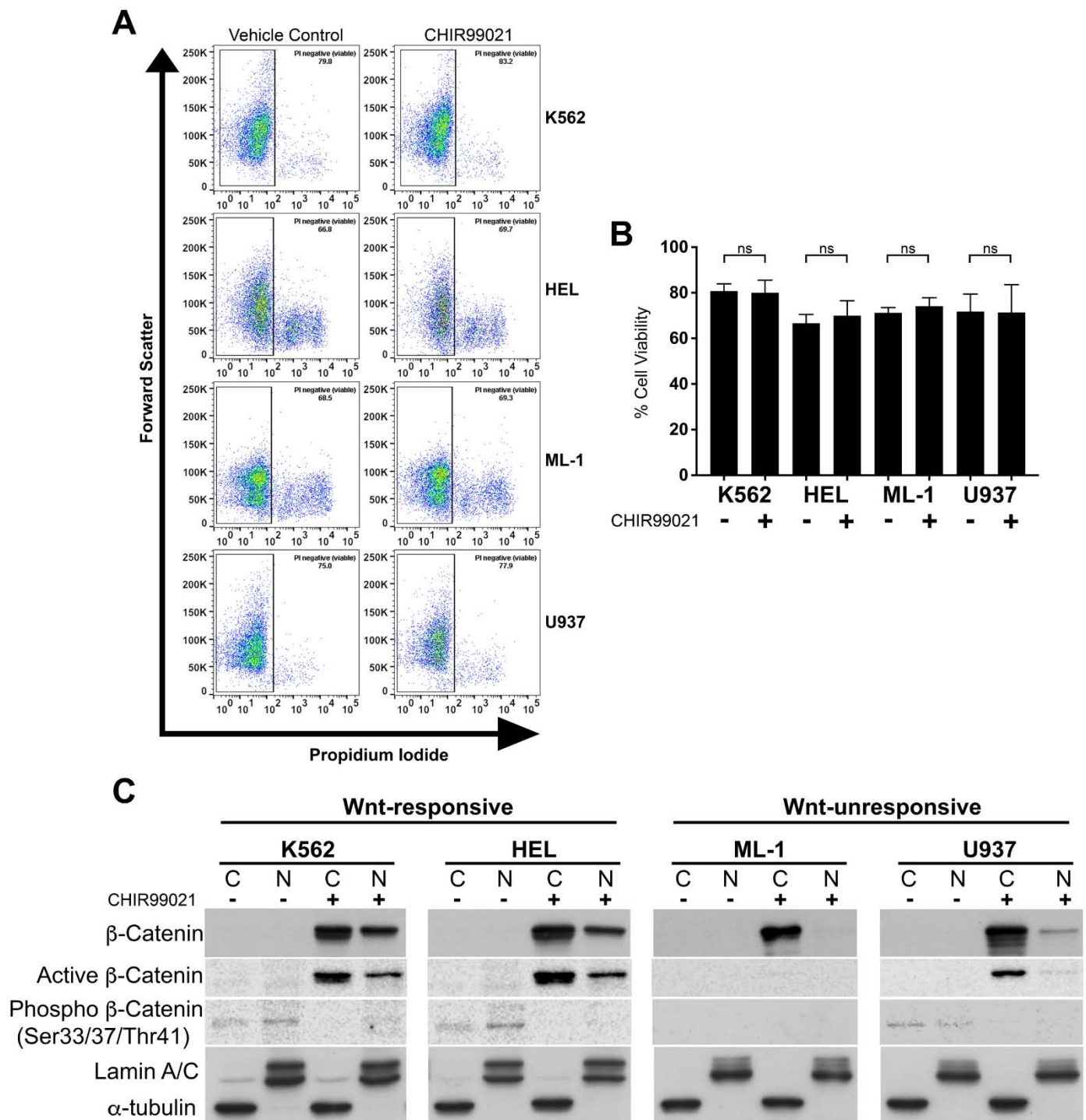MLL = *Mixed-lineage leukemia*
NPM1 = *Nucleophosmin*
FLT3 = *Fms-like tyrosine kinase 3*
RUNX1 = *Runt-related transcription factor 1*
GATA2 = *GATA Binding Protein 2*
WHO = World Health Organisation
n/a = not available

Supplementary Figure S1. Myeloid cell line viability and β-catenin phosphorylation variant expression in response to GSK3 inhibition. (**A**) Representative flow cytometric pseudocolor plots showing propidium staining for K562, HEL, ML-1 and U937 cells following 16hr 5μM CHIR99021 treatment. Percentage of events falling into PI negative gate (viable) are given in upper right of each plot. (**B**) Summary showing the percentage cell viability for each myeloid cell line following 16hr 5μM CHIR99021 treatment. (**C**) Representative immunoblots showing total β-catenin, active (non-phosphorylated) β-catenin and phosphorylated β-catenin (Ser33/37/Thr41) subcellular-localization in myeloid cells following CHIR99021 treatment (GSK3β inhibitor). Lamin A/C and α-tubulin indicate the purity/loading of the nuclear (N) and cytosol (C) fractions respectively. Data represents mean±1 SD, *n*=3, ns=not significant.
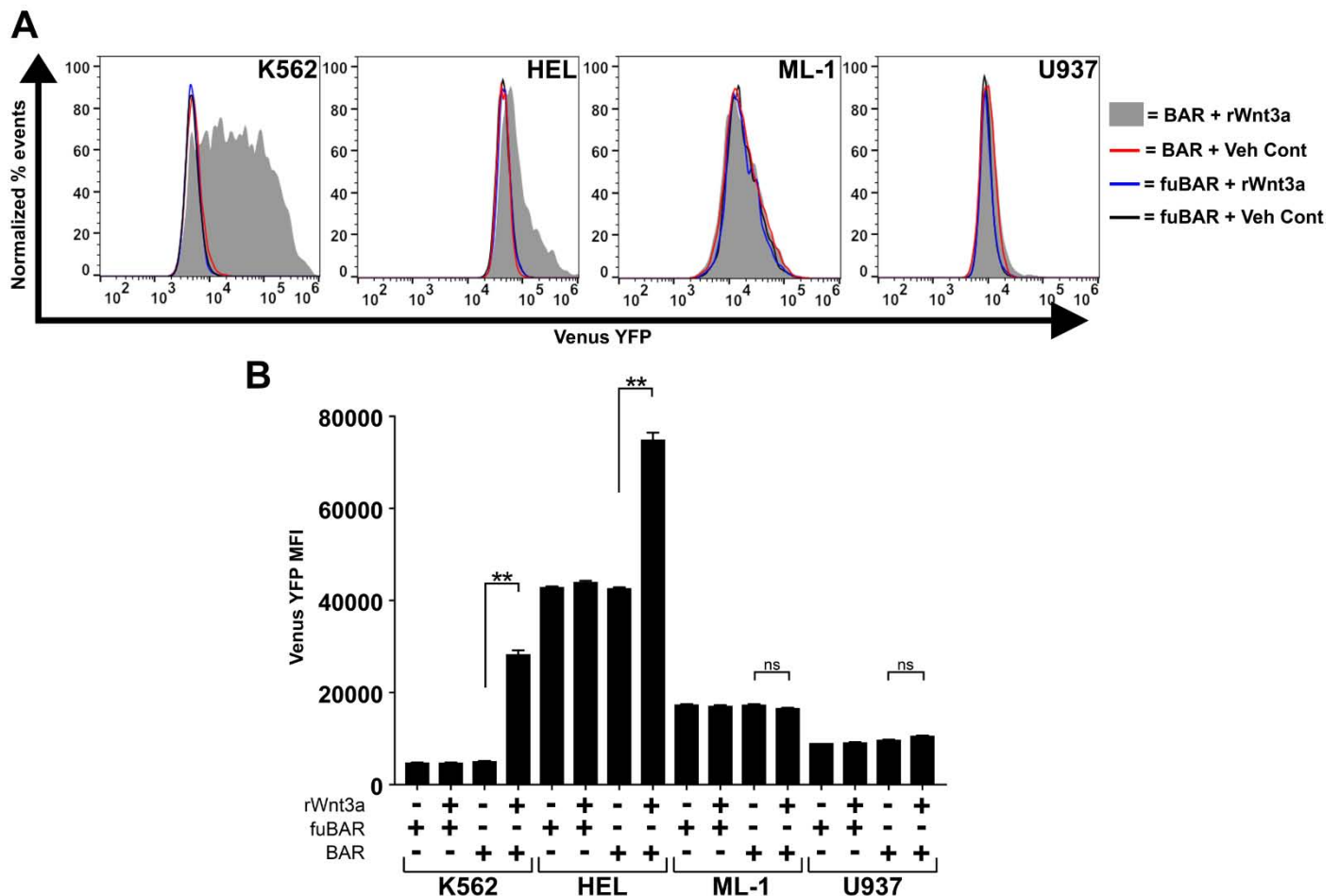
Supplementary Figure S2. Myeloid leukemia cell lines exhibit a heterogeneous response to Wnt stimulation with Wnt3a. (**A**) Representative flow cytometric histograms showing intensity of the TCF-dependent expression of YFP from the 'β-catenin activated reporter' (BAR) reporter, or negative control 'found unresponsive β-catenin activated reporter' (fuBAR) control (containing mutated promoter binding sites) following treatment with rWnt3a/vehicle control (PBS/0.1% BSA) for 16hr. (**B**) Summary showing the median fluorescence intensity generated from the BAR/fuBAR reporters in myeloid cell lines treated ± rWnt3a. Data represents mean±1 SD, statistical significance is denoted by **P<0.01 and ns=not significant.
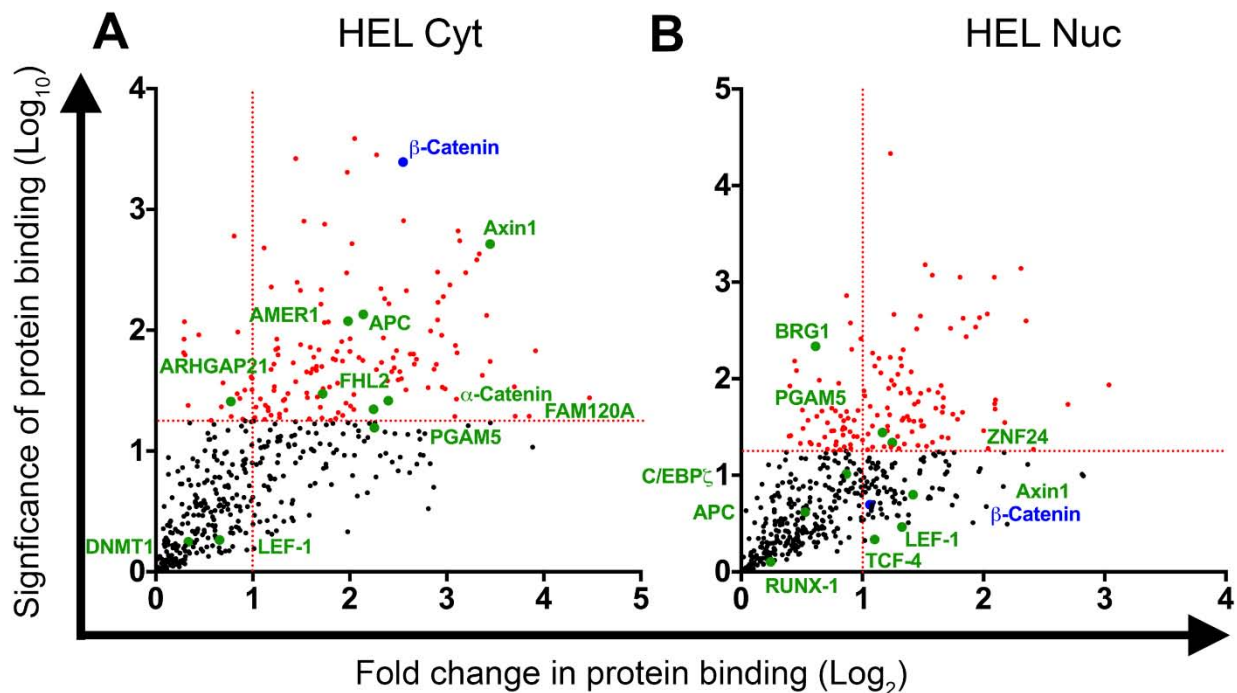
Supplementary Figure S3. Proteomics analyses reveal rich β-catenin interaction networks in Wnt-responsive HEL cells. Scatter plots showing summary of β-catenin protein interactions detected in HEL (**A**) cytosolic, and (**B**) nuclear fractions (*n*=3). Vertical dashed red line indicates the threshold for 2-fold change in protein binding at $\log_2$ (=1) relative to IgG Co-IP. Horizontal red line represents threshold for significant interactions at *p*=0.05 on $\log_{10}$ scale (=1.3). Highlighted red dots indicate all statistically significant interactions, blue dot indicates position of β-catenin bait and green highlighted events/labels indicate known enriched interactions/associations for β-catenin. Remaining black dots represent other proteins detected in the MS analysis. Fold change values less than 0 are not shown because these likely represent contaminants (see Supplementary material).

Supplementary Table S2. List of novel β-catenin interactions observed in K562 and ML1 cytosolic and nuclear fractions. Significant proteins only are shown, and specificity was defined as proteins detected in 10% or less of the 411-affinity purified mass spectrometry datasets present in the CRAPome database. Known interactions were removed from the analysis. Proteins are ranked according to statistical significance of protein binding. Threshold for 2-fold change in protein binding (relative to IgG Co-IP) at $\log_2 = 1$, whilst threshold for significant interactions at $p=0.05$ on $\log_{10}$ scale = 1.3.

Significance of protein binding (-Log10 *t*-test p value)	Fold change in protein binding (Log2)	Gene name	CRAPome frequency (/411)
		K562 Cytosol	
3.77	3.01	CPEB4	1
2.95	1.52	DDX20	40
2.78	1.95	MRPS17	11
2.58	3.03	PRKRA	23
2.42	1.78	IGHMBP2	8
2.35	0.41	APOBEC3B	9
2.25	2.13	MRPS23	21
2.22	1.99	TRIM25	29
2.09	0.72	ABCF2	24
2.08	2.30	DHX36	23
2.07	0.56	MRPL1	13
2.06	1.85	FASTK	0
2.01	2.78	ZC3H7A	5
2.01	1.89	PPHLN1	32
1.95	1.62	EIF2AK2	14
1.93	0.98	FLJ13612	24
1.91	1.02	MRPS15	15
1.89	2.07	UPF1	35
1.87	1.08	MRPL11	11
1.87	0.33	DDX24	40
1.86	1.42	ZC3H7B	2
1.82	2.06	MRPL2	22
1.81	1.37	ZNF346	2
1.78	1.48	MRPL27	14
1.74	0.69	MBD3	32
1.74	0.46	NOL11	25
1.70	1.01	TOE1	21
1.69	1.88	MSI2	13
1.68	0.96	XRN1	26
1.62	2.39	AP2M1	21
1.61	3.12	ZCCHC3	8
1.61	1.18	MRPS22	32
1.58	2.57	DROSHA	10
1.57	0.36	FYTTD1	13
1.53	2.73	MRPL15	13
1.53	0.46	NXF2B	0
1.51	1.19	FAM83A	0
1.51	2.09	PURA	27
1.46	0.74	HNRNPLL	21
1.43	0.66	PNAS 3	34
1.43	2.00	PCM1	31
1.43	1.17	APOBEC3F	17
1.41	1.64	CELF1	10
1.40	1.26	LARP1B	36
1.37	1.72	BMP2K	0
1.36	1.98	MRPS34	24
1.35	1.42	RBM45	2
1.34	0.61	ASCC3	39
1.33	2.60	STAU2	32
1.32	2.27	AP2A1	24
1.31	2.14	AP2M1	21
1.31	1.37	RBM7	23
1.30	0.68	WDR76	8
1.28	3.01	APOBEC3G	0
1.27	1.51	MRPS2	19
1.26	1.66	ARHGAP21	21
1.26	1.76	DAP3	41
		K562 Nucleus	
2.17	0.47	LIN28B	10
2.06	0.42	DDX24	40
2.01	0.58	ZCCHC9	2
1.96	0.71	UTP20	12

|			
1.86	0.28	PRC1	22
1.81	0.48	MRPS24	2
1.65	0.50	POP1	40
1.61	0.56	INTS6	1
1.60	0.27	ABCF2	24
1.56	0.61	DECR1	15
1.54	1.58	RBM45	2
1.52	1.35	NCOA5	19
1.50	0.59	UTP3	23
1.45	0.54	DAP3	41
1.41	0.51	NOL9	34
1.38	0.34	RRP1B	21
1.35	0.61	MYBBP1A	3
1.32	0.48	HNRPUL1	0
1.30	0.89	HNRNPH1	30
1.30	0.41	DDX10	14
1.27	0.39	GNL2	32
1.26	0.42	MBD3	13
1.26	0.29	EXOSC9	2
1.25	0.29	TIMM21	0
ML1 Cytosol			
2.62	2.56	KRT34	28
2.60	0.82	PPIF	28
2.58	1.14	CLTB	14
2.12	0.30	ADRBK1	0
1.79	0.43	ATP6V1E1	16
1.75	0.52	NXF1	38
1.55	0.43	RBM15	40
1.52	0.60	PIK3R1	5
1.44	0.28	RAB5B	40
1.41	0.39	HMGN5	9
1.32	1.07	CENPV	26
1.26	1.22	FABP5	38
ML1 Nucleus			
2.41	0.06	INPP5D	0
1.79	0.92	PNP	36
1.44	0.40	TMX1	23
1.43	0.18	RBM15	40
1.42	0.31	HBS1L	32
1.41	0.75	CDV3	26
1.34	0.30	BUD31	28
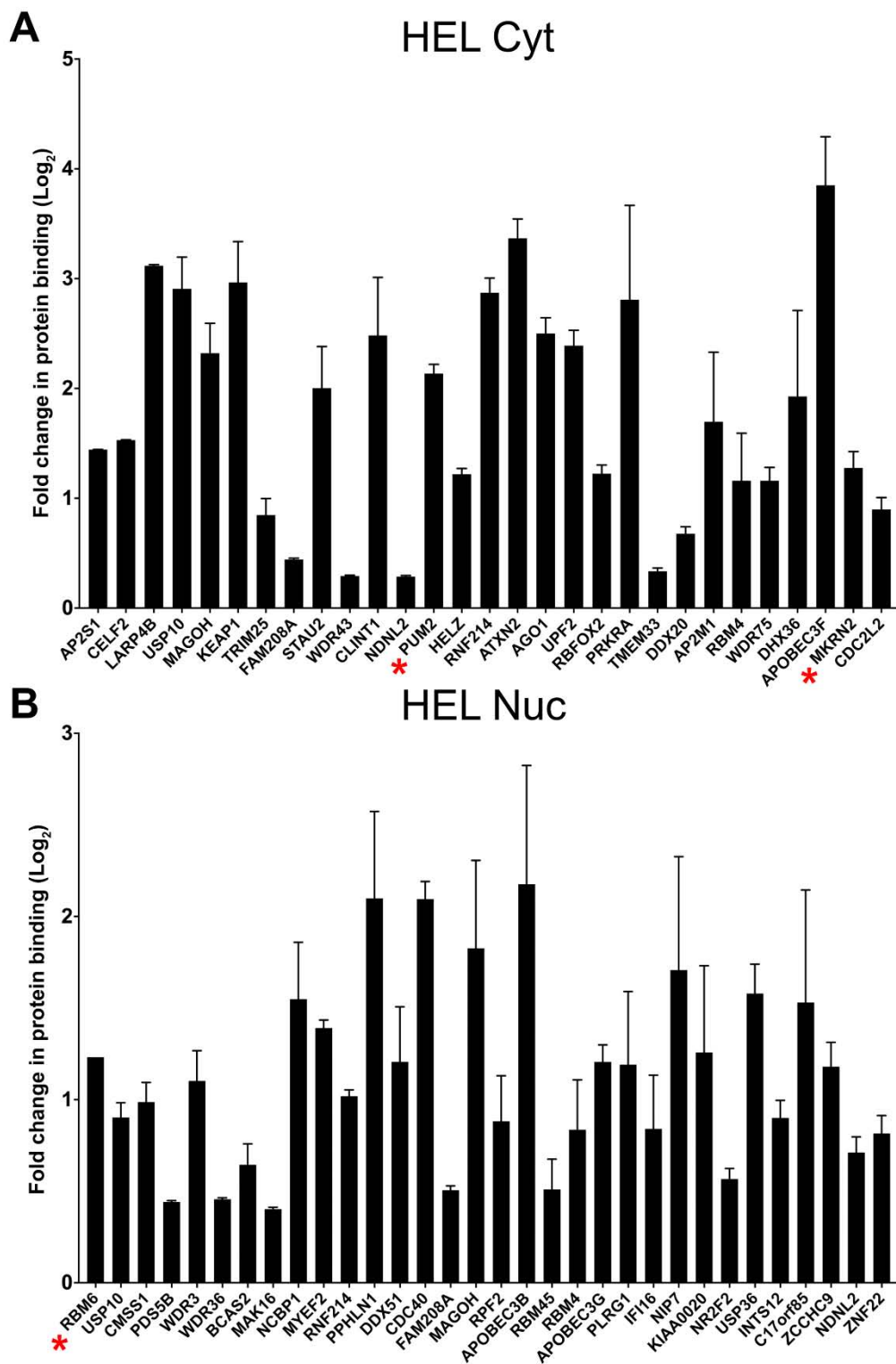
Supplementary Figure S4. Mass spectrometric analyses identify putative novel interaction partners for β-catenin in HEL cells. Bar graphs summarising the average fold change in protein binding (relative to matched IgG co-IP) for novel β-catenin interactions observed in HEL (**A**) cytosolic and (**B**) nuclear fractions. Significant proteins only are shown (red dots in Supplementary Figure S1 panels) with a frequency on the CRAPome database of ≤10% and known interactions were removed. Red asterisks represent proteins of particular significance to myeloid leukemias and/or Wnt signaling (discussed further in results section). Proteins are ranked along X-axis according to statistical significance (left = most significant); see also Supplementary Table S3.

Supplementary Table S3. List of novel β-catenin interactions observed in HEL cytosolic and nuclear fractions. Significant proteins only are shown, and specificity was defined as proteins detected in 10% or less of the 411-affinity purified mass spectrometry datasets present in the CRAPome database. Known interactions were removed from the analysis. Proteins are ranked according to statistical significance of protein binding. Threshold for 2-fold change in protein binding (relative to IgG Co-IP) at $\log_2 =1$, whilst threshold for significant interactions at $p=0.05$ on $\log_{10}$ scale $=1.3$.

Significance of protein binding (-Log10 *t*-test p value)	Fold change in protein binding (Log2)	Gene name	CRAPome frequency (/411)
HEL Cytosol			
3.42	1.44	AP2S1	1
2.90	1.53	CELF2	4
2.82	3.12	LARP4B	20
2.48	2.91	USP10	35
2.35	2.32	MAGOH	37
2.28	2.96	KEAP1	30
1.99	0.85	TRIM25	29
1.96	0.44	FAM208A	37
1.93	2.00	STAU2	32
1.93	0.29	WDR43	27
1.83	2.48	CLINT1	40
1.81	0.29	NDNL2	0
1.75	2.14	PUM2	22
1.72	1.22	HELZ	9
1.68	2.87	RNF214	2
1.63	3.37	ATXN2	33
1.59	2.50	AGO1	14
1.58	2.39	UPF2	0
1.53	1.22	RBFOX2	14
1.52	2.81	PRKRA	23
1.38	0.33	TMEM33	34
1.37	0.68	DDX20	40
1.36	1.70	AP2M1	21
1.36	1.16	RBM4	33
1.33	1.16	WDR75	15
1.29	1.93	DHX36	23
1.29	3.85	APOBEC3F	17
1.28	1.28	MKRN2	3
1.26	0.90	CDC2L2	39
HEL Nuclear			
4.33	1.23	RBM6	25
2.58	0.90	USP10	35
2.41	0.99	CMSS1	6
2.18	0.44	PDS5B	8
2.13	1.10	WDR3	20
2.08	0.46	WDR36	41
1.98	0.64	BCAS2	40
1.93	0.40	MAK16	13
1.88	1.55	NCBP1	38
1.86	1.39	MYEF2	16
1.82	1.02	RNF214	2
1.78	2.10	PPHLN1	32
1.70	1.21	DDX51	10
1.69	2.09	CDC40	15
1.67	0.51	FAM208A	37
1.65	1.83	MAGOH	37
1.59	0.88	RPF2	27
1.55	2.18	APOBEC3B	9
1.48	0.51	RBM45	2
1.47	0.84	RBM4	33
1.46	1.21	APOBEC3G	0
1.45	1.19	PLRG1	38
1.42	0.84	IFI16	9
1.38	1.71	NIP7	16
1.36	1.26	KIAA0020	16
1.34	0.57	NR2F2	4

| 1.34	1.58	USP36	26
1.32	0.90	INTS12	14
1.30	1.53	C17orf85	22
1.30	1.18	ZCCHC9	2
1.27	0.71	NDNL2	0
1.27	0.81	ZNF22	2
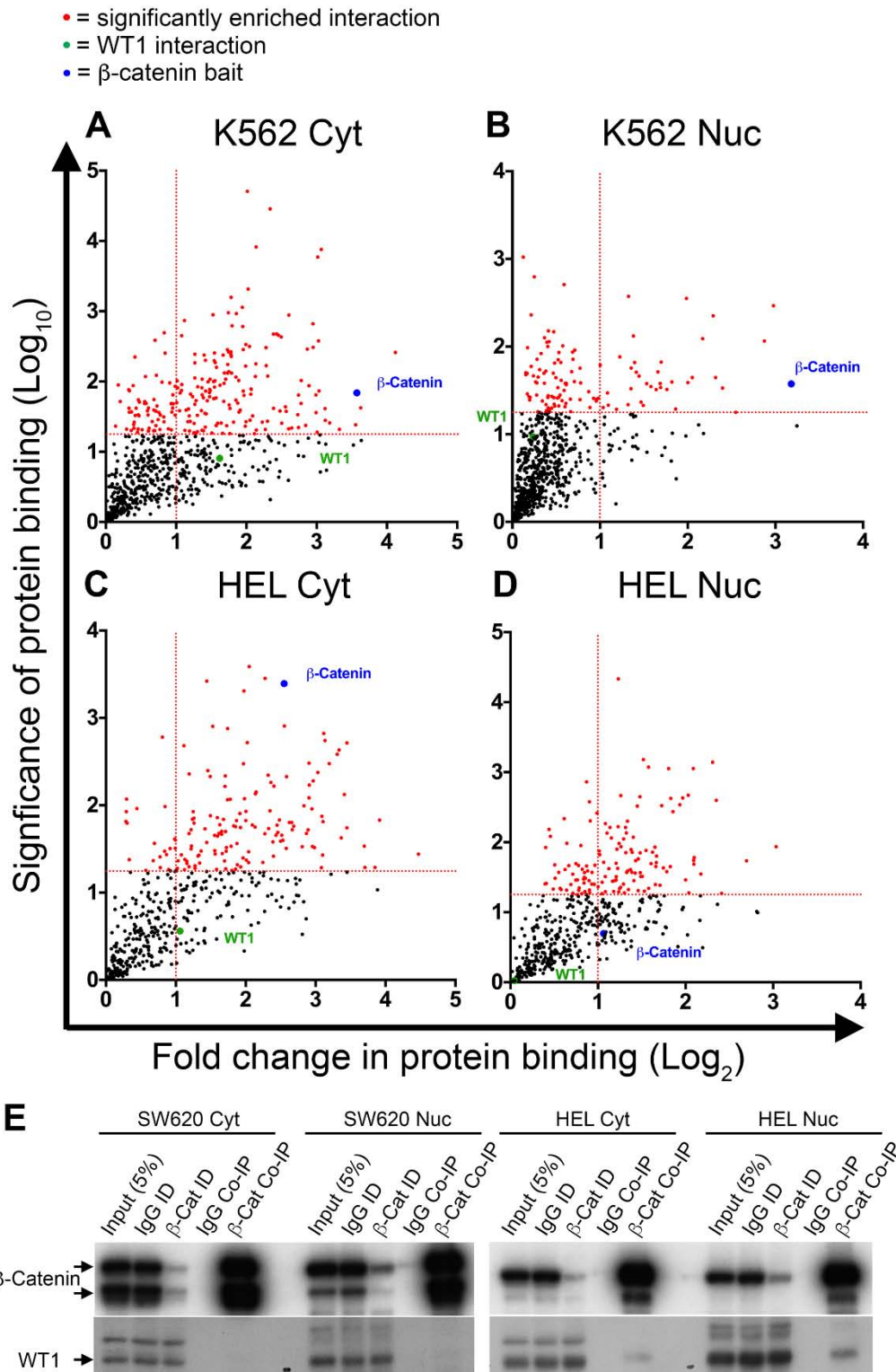
Supplementary Figure S5. Proteomics analyses reveal β-catenin interaction with WT1 in myeloid leukemia cells. Scatter plots showing summary of β-catenin protein interactions detected in (**A**) K562 cytosolic, (**B**) K562 nuclear, (**C**) ML1 cytosolic, and (**D**) ML1 nuclear fractions. Vertical dashed red line indicates the threshold for 2-fold change in protein binding at $\log_2$ (=1) relative to IgG co-IP. Horizontal red line represents threshold for significant interactions at *p*=0.05 on $\log_{10}$ scale (=1.3). Highlighted red dots indicate all statistically significant interactions, blue dot indicates position of β-catenin bait and green dot indicates position of WT1. Remaining black dots represent other proteins detected in the MS analysis. (**E**) Representative immunoblots showing β-catenin and WT1 protein level from β-catenin co-IPs pulled down from the cytosol or nucleus of SW620 or HEL cells (ID=immunodepleted). Note the absence of WT1 detection in SW620 fractions highlighting potential context dependence of interaction.
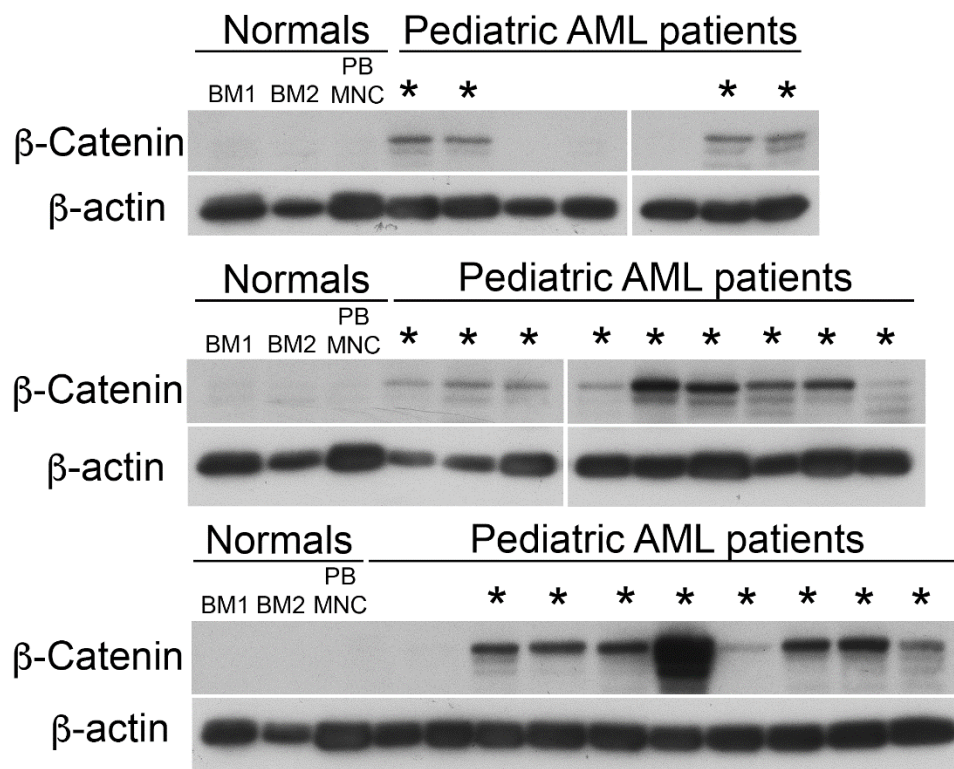
Supplementary Figure S6. Expression of β-catenin protein in pediatric AML samples. Immunoblot screen of 26 primary pediatric AML patient samples showing level of total cell β-catenin compared with normal bone marrow (BM) or peripheral blood mononuclear cells (PB MNC). * samples overexpressing β-catenin protein (~80%) versus levels observed in normal BM or PB MNC. Interestingly, we observed a much higher overall incidence of β-catenin protein overexpression amongst our pediatric AML cohort (Supplemental Figure S4) versus previous estimates for adult AML (~20-60%; see supplemental references).[1,3] This is in keeping with a recent study which examined the molecular landscape of pediatric AML, and found a higher proportion of aberrations which impact Wnt signaling relative to adult AML.[4] *Mixed-lineage leukemia* (*MLL*) gene rearrangements are also more prevalent in childhood AML and this model of leukemogenesis has been shown to require β-catenin for malignant transformation.[5,7] Detection of β-actin was used to assess protein loading.
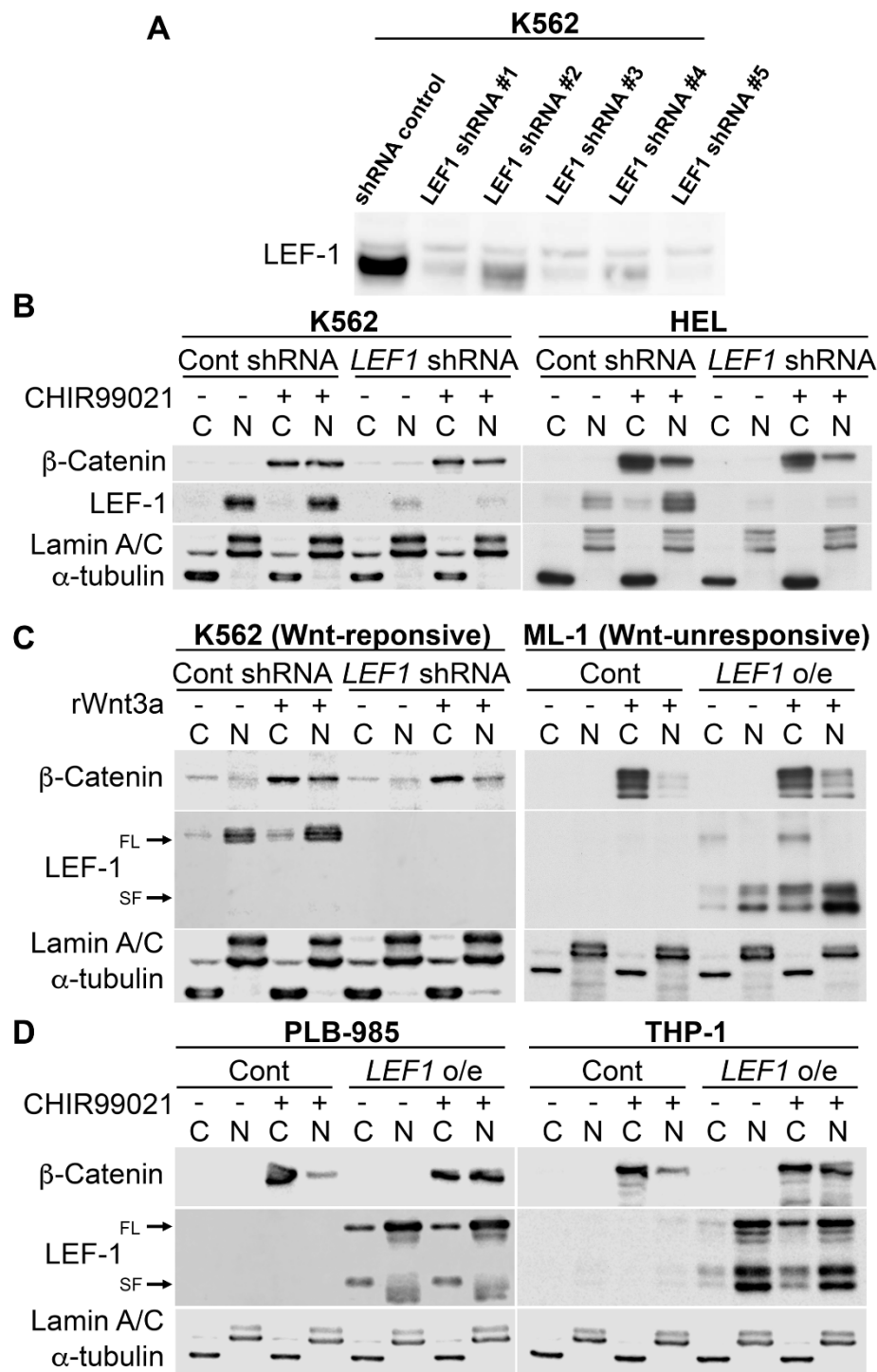
Supplementary Figure S7. Modulation of LEF-1 expression affects relative nuclear β-catenin level. (**A**) Immunoblots showing LEF-1 protein expression level in K562 cells following lentiviral transduction with a panel of 5 human LEF-1 targeted shRNAs (#1 = TRCN0000-020163, #2 = -413476, #3 = -418104, #4= -428178 and #5= -428355). Since LEF-1 shRNA #5 exhibited optimal LEF-1 protein reduction, this was used preferentially through the study. (**B**) Immunoblots showing the level and subcellular localization of β-catenin in K562/HEL cells in response to an alternative LEF-1 shRNA (#3). (**C**) Immunoblots showing the level and subcellular localization of β-catenin in representative Wnt-responsive cells (K562; exhibiting LEF-1 knockdown) and Wnt-unresponsive cells (ML-1; exhibiting LEF-1 overexpression) following Wnt3a exposure. The positions of full-length (FL) and short-forms (SF) of LEF-1 protein on the blot are indicated by arrows. (**D**) Immunoblots showing the level and subcellular localization of β-catenin in PLB-985 and THP-1 cells in response to control/*LEF1* overexpression (o/e) ± 16 hr CHIR99021 treatment. Lamin A/C and α-tubulin were used to assess fraction purity and protein loading.
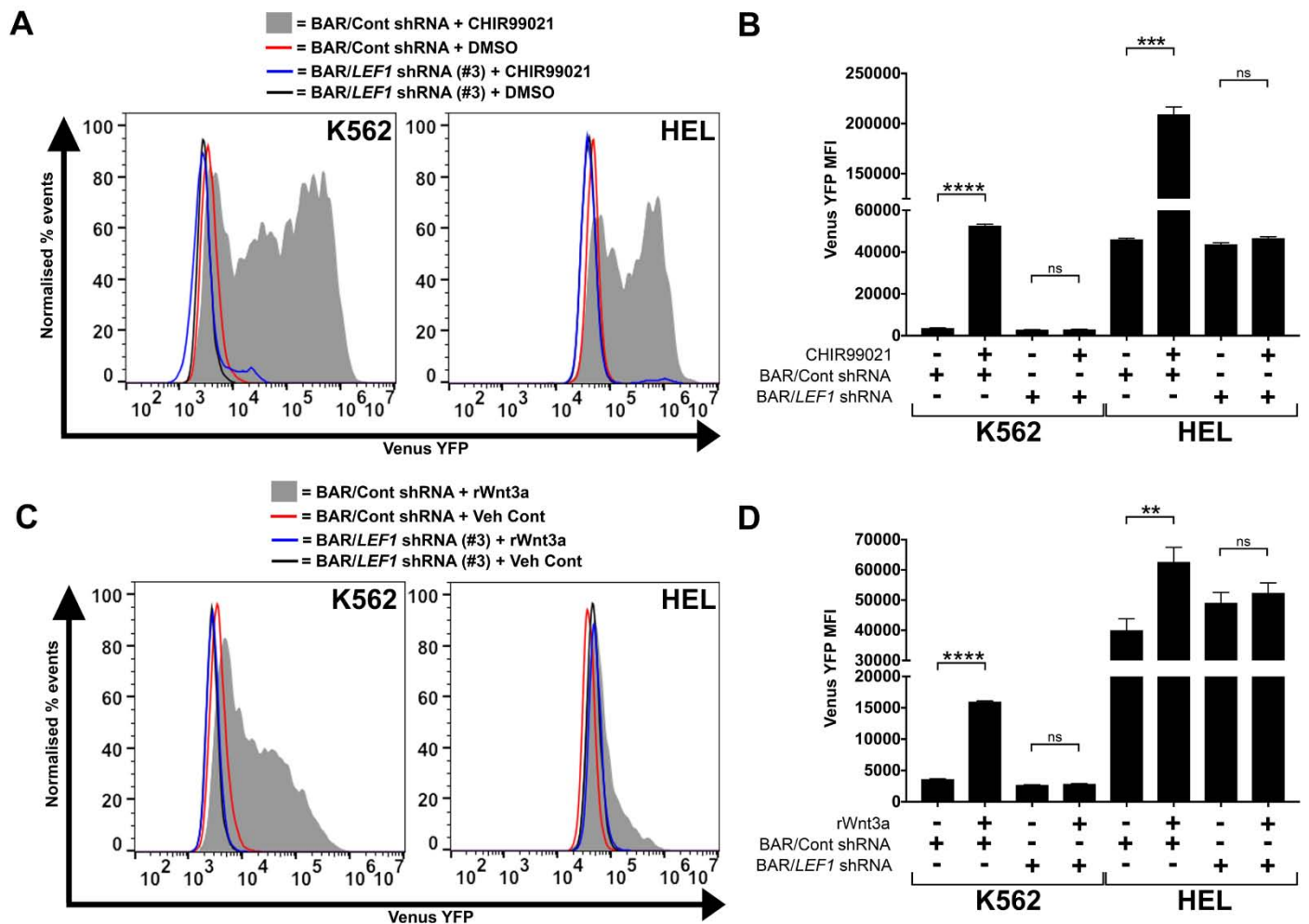
Supplementary Figure S8. Modulation of LEF-1 expression affects downstream Wnt signalling. (**A**) Representative flow cytometric histograms showing intensity of the TCF reporter (BAR) in K562 and HEL cells treated with an alternative *LEF1* shRNA (#3) ± CHIR99021. (**B**) Summary data showing the median fluorescence intensity generated from the BAR reporter in K562 and HEL cells treated with an alternative *LEF1* shRNA (#3) ± CHIR99021. (**C**) Representative flow cytometric histograms showing intensity of the BAR reporter in K562 and HEL cells treated with an alternative *LEF1* shRNA (#3) ± rWnt3a. (**D**) Summary data showing the median fluorescence intensity generated from the BAR reporter in K562 and HEL cells treated with an alternative *LEF1* shRNA (#3) ± rWnt3a. Data represents mean±1 SD, statistical significance is denoted by **$P<0.01$, ***$P<0.001$, ****$P<0.0001$ and ns=not significant.
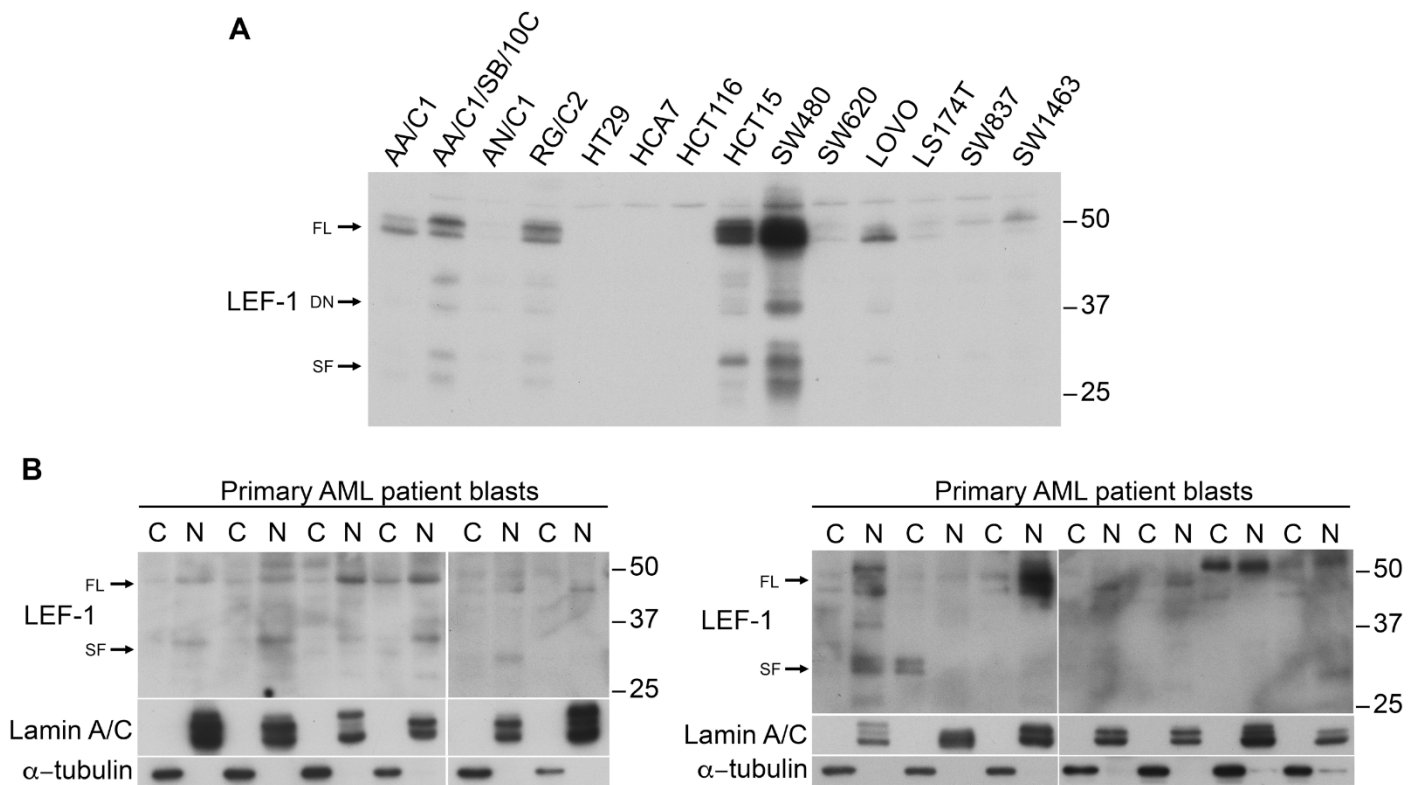
Supplementary Figure S9. Short forms of LEF-1 protein are observed in CRC cell lines and primary AML samples. (**A**) Immunoblot screen of 14 colorectal adenoma or cancer cell lines showing abundance of different LEF-1 protein forms. The positions of full-length (FL), dominant-negative isoforms (DN) and short-forms (SF) of LEF-1 protein are indicated by arrows. The loading control for this blot has previously been published elsewhere.[8] (**B**) Extended immunoblots showing the cytosolic and nuclear expression of LEF-1 protein forms in the primary AML patient samples featured in Figure 5. Lamin A/C and α-tubulin were used to assess fractionation efficiency and equal protein loading.

1.   Chen CC, Gau JP, You JY, Lee KD, Yu YB, Lu CH, *et al.* Prognostic significance of beta-catenin and topoisomerase IIalpha in de novo acute myeloid leukemia. *AmJHematol* 2009; **84**(2)**:** 87-92.

2.   Ysebaert L, Chicanne G, Demur C, De TF, Prade-Houdellier N, Ruidavets JB, *et al.* Expression of beta-catenin by acute myeloid leukemia cells predicts enhanced clonogenic capacities and poor prognosis. *Leukemia* 2006; **20**(7)**:** 1211-1216.

3.   Xu J, Suzuki M, Niwa Y, Hiraga J, Nagasaka T, Ito M, *et al.* Clinical significance of nuclear non-phosphorylated beta-catenin in acute myeloid leukaemia and myelodysplastic syndrome. *BrJHaematol* 2008; **140**(4)**:** 394-401.

4.   Bolouri H, Farrar JE, Triche T, Jr., Ries RE, Lim EL, Alonzo TA, *et al.* The molecular landscape of pediatric acute myeloid leukemia reveals recurrent structural alterations and age-specific mutational interactions. *Nat Med* 2017.

5.   Wang Y, Krivtsov AV, Sinha AU, North TE, Goessling W, Feng Z, *et al.* The Wnt/beta-catenin pathway is required for the development of leukemia stem cells in AML. *Science* 2010; **327**(5973)**:** 1650-1653.

6.   Yeung J, Esposito MT, Gandillet A, Zeisig BB, Griessinger E, Bonnet D, *et al.* beta-Catenin mediates the establishment and drug resistance of MLL leukemic stem cells. *Cancer Cell* 2010; **18**(6)**:** 606-618.

7.   Dietrich PA, Yang C, Leung HH, Lynch JR, Gonzales E, Liu B, *et al.* GPR84 sustains aberrant beta-catenin signaling in leukemic stem cells for maintenance of MLL leukemogenesis. *Blood* 2014; **124**(22)**:** 3284-3294.

8.   Legge DN, Shephard AP, Collard TJ, Greenhough A, Chambers AC, Clarkson RW, *et al.* BCL-3 enhances β-catenin signalling in colorectal tumour cells promoting a cancer stem cell phenotype. *bioRxiv* doi: 10.1101/178004.

Supplementary Methods

Cross-linking of antibodies for co-immunoprecipitation

For co-immunoprecipitation, 8µg of β-catenin (Clone 14)/IgG (Clone MOPC-31C) antibody (Becton Dickinson, Oxford, UK) was crosslinked to Protein G Dynabeads® (Thermo Fisher Scientific, Loughborough, UK) for 2h at room temperature. Following washing, bound β-catenin/IgG antibody was crosslinked to Protein G Dynabeads® in coupling buffer (0.2M triethanolamine (Sigma-Aldrich) in PBS with 0.01% Tween-20 (pH9), 20mM Dimethyl pimelimidate dihydrochloride (Sigma-Aldrich) for 1 h at room temperature. Following washing, crosslinked β-catenin/IgG antibody was quenched (50mM ethanolamine (Sigma-Aldrich) in PBS with 0.01% Tween-20) for 30min at room temperature, followed by washing in elution buffer (0.2M glycine (Sigma-Aldrich) pH2.5 with 0.01% Tween-20) to remove uncrosslinked antibody.

TMT Labelling and High pH reversed-phase chromatography

Immunoprecipitated samples (eight samples per experiment) were digested on the beads with trypsin (2.5µg trypsin; 37°C, overnight), labelled with Tandem Mass Tag (TMT) ten-plex reagents according to the manufacturer's protocol (Thermo Fisher Scientific) and the labelled samples pooled. The pooled sample was evaporated to dryness, resuspended in 5% formic acid and then desalted using a SepPak cartridge according to the manufacturer's instructions (Waters, Milford, Massachusetts, USA). Eluate from the SepPak cartridge was again evaporated to dryness and resuspended in buffer A (20 mM ammonium hydroxide, pH 10) prior to fractionation by high pH reversed-phase chromatography using an Ultimate 3000 liquid chromatography system (Thermo Fisher Scientific). In brief, the sample was loaded onto an XBridge BEH C18 Column (130Å, 3.5 µm, 2.1 mm X 150 mm, Waters, UK) in buffer A and peptides eluted with an increasing gradient of buffer B (20 mM Ammonium Hydroxide in acetonitrile, pH 10) from 0-95% over 60 min. The resulting fractions were evaporated to dryness and resuspended in 1% formic acid prior to analysis by nano-LC MSMS.

Nano-LC Mass Spectrometry

High pH RP fractions were further fractionated using an Ultimate 3000 nano-LC system in line with an Orbitrap Fusion Tribrid mass spectrometer (Thermo Scientific). In brief, peptides in 1% (*v/v*) formic acid were injected onto an Acclaim PepMap C18 nano-trap column (Thermo Scientific). After washing with 0.5% (*v/v*) acetonitrile 0.1% (*v/v*) formic acid peptides were resolved on a 250 mm × 75 µm Acclaim PepMap C18 reverse phase analytical column (Thermo Scientific) over a 150 min organic gradient, using 7 gradient segments (1-6% solvent B over 1 min, 6-15% B over 58 min, 15-

32% B over 58 min, 32-40% B over 5 min, 40-90% B over 1 min, held at 90% B for 6 min and then reduced to 1% B over 1 min) with a flow rate of 300 nl/min. Solvent A was 0.1% formic acid and Solvent B was aqueous 80% acetonitrile in 0.1% formic acid. Peptides were ionized by nano-electrospray ionization at 2.0kV using a stainless-steel emitter with an internal diameter of 30 μm (Thermo Scientific) and a capillary temperature of 275°C. All spectra were acquired using an Orbitrap Fusion Tribrid mass spectrometer controlled by Xcalibur 2.0 software (Thermo Scientific) and operated in data-dependent acquisition mode using an SPS-MS3 workflow. FTMS1 spectra were collected at a resolution of 120 000, with an automatic gain control (AGC) target of 200 000 and a max injection time of 50ms. Precursors were filtered with an intensity threshold of 5000, according to charge state (to include charge states 2-7) and with monoisotopic precursor selection. Previously interrogated precursors were excluded using a dynamic window (60s +/-10ppm). The MS2 precursors were isolated with a quadrupole mass filter set to a width of 1.2m/z. ITMS2 spectra were collected with an AGC target of 10 000, max injection time of 70ms and CID collision energy of 35%. For FTMS3 analysis, the Orbitrap was operated at 50 000 resolution with an AGC target of 50 000 and a max injection time of 105ms. Precursors were fragmented by high energy collision dissociation (HCD) at a normalized collision energy of 60% to ensure maximal TMT reporter ion yield. Synchronous Precursor Selection (SPS) was enabled to include up to 5 MS2 fragment ions in the FTMS3 scan.

Mass spectrometry Data Analysis
The raw data files were processed and quantified using Proteome Discoverer software v1.4 (Thermo Scientific) and searched against the UniProt Human database (134169 entries downloaded 18/4/2016) using the SEQUEST algorithm. Peptide precursor mass tolerance was set at 10ppm, and MS/MS tolerance was set at 0.6Da. Search criteria included oxidation of methionine (+15.9949) as a variable modification and carbamidomethylation of cysteine (+57.0214) and the addition of the TMT mass tag (+229.163) to peptide N-termini and lysine as fixed modifications. Searches were performed with full tryptic digestion and a maximum of 1 missed cleavage was allowed. The reverse database search option was enabled and all peptide data was filtered to satisfy false discovery rate (FDR) of 1%.

β-Catenin and LEF-1 densitometry
Densitometry was performed using ImageJ software v2.0.0-rc-43/1.51s (National Institutes of Health, Bethesda, MD, USA) and arbitrary densitometric units used to calculate relative nuclear β-catenin/LEF-1 localization. Relative percentage nuclear localization was calculated by normalizing the β-catenin or LEF-1 protein level to the α-tubulin or lamin A/C protein level present in the

respective cytosolic or nuclear fraction, followed by calculation of the nuclear β-catenin or LEF-1 present as a proportion of the total β-catenin or LEF-1 level.

Supplementary MS data (see associated Excel file).

Raw and processed tandem mass tag (TMT) mass spectrometry data obtained from β-catenin co-IP's from K562, HEL, ML-1 and SW620 cytoplasm and nuclear fractions. These data can also be found deposited to the ProteomeXchange Consortium (http://proteomecentral.proteomexchange.org) via the PRIDE partner repository with the dataset identifier PXD009305. Parameter definitions and data sheet types are explained within the first sheets of the excel file.